PERGAMON

Applied Radiation and Isotopes 50 (1999) 811–833

Applied Radiation and Isotopes

Chemical digestion and radionuclidic assay of TiNi-encapsulated ^{32}P intravascular brachytherapy sources

R. Collé *

Physics Laboratory, National Institute of Standards and Technology, Gaithersburg, MD 20899-8462, USA

Received 24 August 1998; accepted 31 August 1998

Abstract

A very quantitative, destructive assay procedure was devised for accurately measuring the ^{32}P activity content of TiNi-encapsulated intravascular brachytherapy sources and was applied to four different sources (termed 'seeds') which were developed and provided by Guidant Intravascular Intervention (formerly NeoCardia). These seeds are intended for use in the prophylactic treatment of restenosis following balloon angioplasty in heart-disease patients. The assays involved the dissolution of the TiNi jacket, extraction of the activity from the internal ^{32}P-containing source material, quantitative solution transfers, and a gravimetrically-based dilution; followed by liquid scintillation (LS) spectrometry of the resulting master solution with ^{3}H-standard efficiency tracing using composition-matched LS cocktails. The LS spectrometry utilized a previously-developed method for resolving the always-present ^{33}P impurity. The protocol included provisions for accounting for all possible losses of ^{32}P in the digestion procedure (based on radiochemical tracing experiments), for any unrecovered activity in the remaining source material, and for any residual activity in the solution-transfer and containing vessels. Sections of the TiNi jackets adjacent to the cut-off active seed portions were also assayed for any contained activity. Such destructive assays were required for relating measurements of the absorbed dose spatial distribution for the seeds to theoretic dose modelling and for establishing calibration factors for subsequent non-destructive radionuclidic measurements on the seeds. Published by Elsevier Science Ltd.

1. Introductory considerations

1.1. On the use of intravascular brachytherapy sources for the prophylactic treatment of restenosis

Heart diseases are the leading causes of both morbidity and mortality in the western world. Based on 1994 estimates by the American Heart Association, nearly 60 million Americans alone have one or more of its forms, of which coronary-artery disease causes nearly a half-million deaths per year and is the single leading cause of death in the US today (AHA, 1997).

This cardiovascular disease is caused by atherosclerotic narrowing (or stenosis) of the heart's arteries, which is likely to produce angina pectoris, heart attack, or both. Balloon angioplasty is one invasive procedure that is used for widening the coronary arteries. As a result, approximately 400,000 angioplasties are now performed annually in the US. However, one third or more of patients undergoing angioplasty procedures have restenosis, or renewed narrowing, of the widened artery within six months of the treatment and restenosed arteries may then have to undergo yet another angioplasty procedure. Restenosis is believed to occur because of reclosing of the artery by scar-tissue formation during the post-angioplasty healing process. Restenosis may also occur after coronary-artery-bypass graft operations. This type of heart surgery is done to 'bypass', or reroute blood around clogged arteries to improve the supply of oxygenated blood to the heart. In this case, the stenosis might occur in the blood-vessel segments that were transplanted and

* Tel.: +1-301-975-5527; fax: +1-301-926-7416; e-mail: rcolle@nist.gov

0969-8043/99/$ - see front matter Published by Elsevier Science Ltd.
PII: S0969-8043(98)00167-5

grafted. As for other stenosed arteries, they may have to undergo angioplasty or atherectomy to reopen them.

Extensive research is currently underway to investigate ways to prevent restenosis. In addition to the placement of coronary stents (expandable supports that are placed inside arteries that restenose repeatedly) in conjunction with angioplasty, recent preclinical studies indicate that radiation doses in the range of 10 to 30 Gy through the temporal placement of intravascular brachytherapy sources may substantially reduce the rate of occurrence of restenosis. Inasmuch as the US societal cost of restenosis has been estimated to be between 800 million and two billion dollars per year (CIRMS, 1998), there is a tremendous ongoing effort within the cardiology and radiation oncology communities to more fully research the use of intravascular brachytherapy sources for the prophylactic treatment of restenosis.

Several high-energy beta emitters have been proposed as suitable candidate radionuclides for such intravascular brachytherapy sources (Coursey et al., 1994, 1998). For example, Guidant Vascular Intervention (Houston, TX), formerly NeoCardia, has developed and has been investigating the use of a TiNi-encapsulated ^{32}P source (Lott, 1997). The National Institute of Standards and Technology (NIST), in collaboration with Guidant, has performed the necessary radiochromic-film dosimetry (Soares, 1997) and Monte-Carlo-calculational dose modelling (Seltzer, 1997) to establish dose profiles. At the same time, NIST initiated efforts to perform destructive radionuclidic assays that could be used to relate the ^{32}P activity content of the Guidant source to these measured and calculated absorbed dose spatial distributions. This paper describes the results of that latter work.

1.2. On the importance and need for destructive, radionuclidic assays of the sources

The importance of these radionuclidic assays is illustrated in the schematic of Fig. 1. The need for accurate determinations of the activity content of brachytherapy sources by destructive (chemically-digestive), analytical methods may be considered from at least five perspectives.

Firstly, the activity content of the sources must be known in order to unequivocally relate measurements and calculations of the absorbed dose spatial distributions. These dose determinations are critical for evaluating the efficacy of the radiation-induced prevention of restenosis and for the meaningful interpretation of results from various preclinical studies and clinical trials. Uniform and consistently-determined dose profiles are particularly important since the restenosis

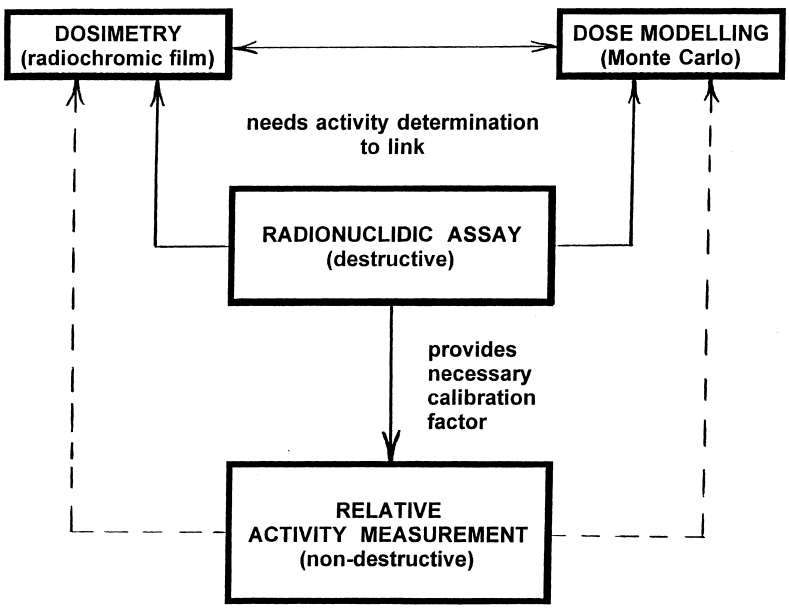

Fig. 1. Illustration of the central role of the destructive radionuclidic assay in providing the necessary link for unequivocally relating absorbed dose spatial distributions from dosimetry to those obtained from dose modelling calculations and for providing calibration factors for subsequent non-destructive activity measurements by relative measurement methods. Refer to the text for additional considerations on the importance and need for these assays.

treatments may use a variety of radionuclides and differing dose delivery systems.

Secondly, the activity contained within a source normally must be determined after the source is manufactured since it is usually exceedingly difficult (if not impossible) to quantitatively fabricate sealed sources with known quantities of starting activity. The small-scale dimensions of intravascular brachytherapy sources and their need to be chemically inert within the human body, only exacerbate the difficulties.

Thirdly, relative activity measurements, e.g. with re-entrant ionization-chamber-based instruments (often described in the medical community by the misnomer 'dose calibrators'), cannot be performed in the absence of pre-determined calibration factors (like a dose calibrator 'dial setting') for the instruments. Such calibration factors can only be established by relating the instrument's relative response to some previously known activity determination for the source.

Fourthly, sealed sources of single-transition, pure β-emitting nuclides like ^{32}P have no distinctive, external, radiative signatures (e.g. monoenergetic γ rays) or coincident transitions which precludes use of measurement techniques like γ-ray spectrometry or more exacting coincidence measurement methods. Hence, the radionuclidic content of these sources must be assayed by destructive means.

Lastly, one cannot ignore the legal and commercial considerations. Governmental regulatory authorities, be they agencies concerned with the licensing of the use of radioactive materials (like the US Nuclear Regulatory Commission) or those concerned with the efficacious use of medical devices (like the US Food and Drug Administration's Center for Devices and Radiological Health), normally require that manufacturers and users of sealed sources have knowledge of their activity content. Furthermore, for equity-in-trade purposes, the high cost of sufficiently-pure radioactive materials that are used to prepare the sources and the vast potential market for the use of these sources in the global medical marketplace dictates that they have activity contents that are based on accurate and internationally-compatible measurements.

As shown by the interrelationships of Fig. 1, the destructive assays, performed and described herein, served as the necessary link for relating the dose measurements and calculations and for providing calibration factors for subsequent activity determinations by relative non-destructive measurement methods.

1.3. On the decay and radionuclidic assay of ^{32}P

The nuclide ^{32}P, with a half-life of $T_{32} = 14.262 \pm 0.014$ d, decays by pure β-emission to the ground state of ^{32}S by an allowed transition ($J^{\pi} = 1^{+} \rightarrow 0^{+}$) having a well-known β-spectrum maximum endpoint energy of $E_{\beta(\max)} = 1710.3 \pm 0.6$ keV and a number-weighted mean energy of $E_{\beta(\text{mean})} = 694.9 \pm 0.3$ keV (ENSDF, 1997). Determinations of the activity for nuclides that decay by pure β-emission to the ground state of their daughters are amongst the more difficult within the realm of radionuclidic metrology. The difficulty arises because their emitted β particles in many counting conditions are easily absorbed in counting sources (and thereby require large scattering and absorption-loss corrections) and from the absence of any γ rays and other coincident transitions (which, as noted above, precludes the use of standardization techniques like γ-ray spectrometry or primary β–γ coincidence methods). In the past decade, considerable progress has been made in applying liquid scintillation (LS) spectrometry to the assay of such radionuclides through 4π detection of the β particles. The overall LS detection efficiency for high-energy β emitters like ^{32}P is very high and approaches nearly 100% for moderately quenched LS cocktails.

Most commercial supplies of ^{32}P invariably contain a longer-lived ($T_{33} = 25.34 \pm 0.12$ d) impurity of ^{33}P. The impurity ratio I, for the ^{32}P-to-^{33}P activities, is typically of the order of $I \leq 0.008$ for relatively fresh supplies that have not undergone substantial decay. With the passage of time t, the initial I increases by a growth factor of $\exp[(\lambda_{32} - \lambda_{33})t]$ where $\lambda_{32} = (\ln 2)/T_{32}$ and $\lambda_{33} = (\ln 2)/T_{33}$ are the respective decay constants for ^{32}P and ^{33}P. As a result, assays of ^{32}P normally require an independent or corollary determination of this increasingly attendant impurity.

This impurity determination is somewhat difficult in that ^{33}P is also a pure β emitter having, as previously noted, no other distinctive signature (e.g. γ rays) and because their two decay constants (or half-lifes) differ by less than a factor of two. Furthermore, the usually less abundant ^{33}P impurity has a substantially lower maximum β endpoint energy [$E_{\beta(\max)} = 248.5 \pm 1.5$ keV] compared to that for ^{32}P so that its β spectrum is largely buried underneath the dominant ^{32}P spectrum. The β spectra for ^{32}P and ^{33}P, plotted on logarithmic energy axes, are shown in Fig. 2.

In common practice, these two components are resolved by following the counting rate of a source as a function of time and fitting the background-corrected net rate to a function consisting of the sum of the two ^{32}P and ^{33}P exponentially-decaying terms to extract (as fitted parameters) the ^{32}P and ^{33}P activities. Resolution of the two components is difficult because they have very comparable half-lifes. It becomes an even more difficult task when the impurity ratio I is less than a few percent. In this case, one must perform the measurements over relatively long decay-time intervals to effect an adequate resolution of the two components. An additional complication may arise if the

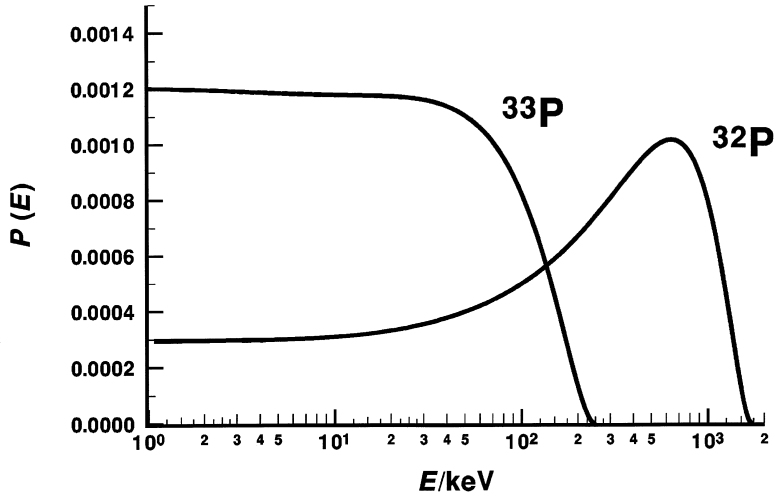

Fig. 2. Theoretical β-particle spectra for ^{32}P and ^{33}P in terms of the probability $P(E)$ of emission of a β particle of energy E (in units of keV) as calculated by the EFFY4 code using the well-known Fermi distribution. The spectra are plotted on logarithmic energy axes with normalizations such that the integral of $P(E)$ over all E is unity.

respective detection efficiencies of the two components vary with time.

One approach for the resolution and assay of such ^{33}P/^{32}P mixtures by LS spectrometry, over a wide variety of conditions, has been described in detail by Collé (1997a). This earlier work demonstrated the utility of using a simple linearizing transform for graphically judging the quality of the available measurement data and of critically evaluating how well the components are resolved.

2. Experimental considerations

2.1. On the TiNi-encapsulated Guidant seeds

Four seeds were submitted to NIST by Guidant for assay. The upper part of Table 1 summarizes the source descriptions, to the extent that their proprietary composition can be disclosed. They consisted of a ^{32}P-containing source material that was encapsulated in a thin-cladded, tubular jacket (of nominal 0.46 mm o.d.) of a TiNi alloy, whose ends had inserted TiNi wires. One end of the tube was sealed by a hemispherical weld of a nominal 1-mm long TiNi wire plug to the TiNi tube. The other end was a long multi-meter wire that would normally be used for insertion into suitable artery catheters. Fig. 3 illustrates the source configuration.

As noted in Table 1, three of the sources had an internal source length of 27 mm, which comprised the ^{32}P-containing 'active' portion of the wires. The fourth (identified as #5) was an earlier prototype which had an 'active' portion of 3 mm. These 'active' portions were located roughly 1 mm from the ends of the long wires. Sections of the long wires containing the 'active' portions were ultimately cut off to varying lengths (Table 1) for the subsequent chemical digestion. Short lengths of the wires adjacent to the 'active' portions were also cut off for assay.

Information on the internal structure and composition of the of the ^{32}P-containing source material in the four sources is proprietary, and cannot be disclosed. The digestion procedure (see below) was devised, however, in consideration of this structure and composition. The internal 'active' portions of all four were somewhat different since the design and fabrication was still under development by Guidant. Nevertheless, they had varying but relatable chemical compositions and physical characteristics. One part of this internal-source material was expected to be nearly chemically impervious. As discussed later, these chemical and physical differences would become manifest in the ease and degree to which the ^{32}P activity could be extracted from the source material in the digestion procedure.

The ^{32}P activities for these sources, as reported by Guidant (Table 1), were very preliminary in nature. Part of this work, of course, was to provide the necessary assay results which were then used to establish suitable calibration factors. These, in turn, were used for in-house quality control measurements and for providing reliable and accurate results for all subsequent non-destructive ^{32}P activity assays. Guidant's initial activity values were based on two kinds of preliminary calibrations (Lott, 1997). The first was obtained from relative ionization current measurements of the seeds in an ionization-chamber-type 'well counter' compared

Table 1
Summary of source descriptions and measurement conditions

Source identification	#5	P-96-32-3	P-97-15-2	P-97-23-6
Source description	A TiNi-encapsulated 'seed' (cut from a long TiNi wire) which contained an internal ^{32}P source; the physical and chemical composition of this ^{32}P source material is proprietary; the ^{32}P source material was encapsulated in a tubular jacket (of nominal 0.46-mm o.d.) of 50:50 TiNi alloy, whose ends had inserted 0.254-mm diameter TiNi wires; one end of the tube was sealed by a hemispherical weld of a TiNi wire plug (of nominal 1-mm length) to the TiNi tube; the other end of the submitted long-wire source was cut for the radionuclidic assay			
Length of internal source (mm)	3	27	27	27
Reported activity (said to be...)	16.07 mCi (594.6 MBq) on 29 January 1996 based on 'well counter' measurements and 10.85 μCi (401.5 kBq) on 25 September 1996 based on an 'LS calibration'[a]	34.5 mCi (1277 MBq) on 1100 EST 26 August 1996	334.14 mCi (12.36 GBq) on 1100 EST 20 February 1997 and 49.12 mCi (1817 MBq) on 0830 EST 2 April 1997[b]	219.3 mCi (8114 MBq) on 1100 EST 6 June 1997
Length of TiNi wire cut off for assay (mm)	previously cut to 21 mm as submitted	35	38	37
Length of adjacent TiNi section assayed (mm)	not available	7	20	17
Calibration method	chemical digestion of the seed, quantitative solution transfers and gravimetric dilution; followed by liquid scintillation (LS) spectrometry of the resulting master solution with ^{3}H-standard efficiency tracing using composition-matched LS cocktails; corrections were applied for residual activities in the undigested portion of the seed and in the solution-transfer tools; the ^{32}P and ^{33}P detection efficiencies were calculated using the EFFY4 code with ^{3}H as the detection-efficiency monitor			
$E_{\beta(max)}$ used in the EFFY4 efficiency computations[c]	^{32}P: 1710.6 ± 0.6 keV; ^{33}P: 248.5 ± 1.5 keV; ^{3}H: 18.594 ± 0.008 keV			
Half-lifes used	^{32}P: 14.262 ± 0.014 d; ^{33}P: 25.34 ± 0.12 d; ^{3}H: 12.33 ± 0.06 a			
Chemical digestion period	2 to 5 December 1996	31 December 1996 to 10 January 1997	25 June 1997 to 17 August 1997	19 to 30 September 1997
LS measurement period	5 to 18 December 1996	10 to 28 January 1997	18 August 1997 to 14 October 1997	1 to 21 October 1997
LS measurement reference time	1200 EST 1 December 1996	1200 EST 14 January 1997	1200 EST 22 August 1997	1200 EST 6 October 1997
Number of LS cocktails used for the assay	one set of 4 cocktails	two sets, one of 5 cocktails and one of 6	three sets, two of 5 cocktails and one of 4	two sets, each of 4 cocktails
ν[d]	54	83	298	158

[a] There is an apparent $\simeq 25\%$ difference in the reported activities between the LS calibration and well counter measurements. Refer to text and Table 8.[b]Based on a ^{32}P half-life of 14.262 d, these two reported activity values are inconsistent by $\simeq 7\%$ (see also Table 8).[c]$E_{\beta(max)}$ is the maximum energy for the beta-particle spectrum. The spectra are assumed to be given by Fermi distributions for allowed transitions.[d]The degrees of freedom ν in the assay regression result is given by the total number of LS cocktails multiplied by the number of measurements on each cocktail minus 2 (for the two fitted parameters).

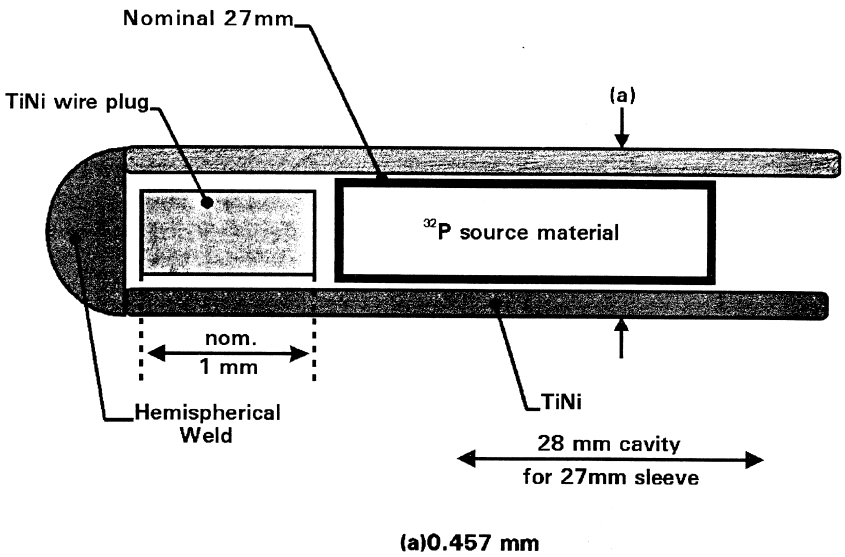

Fig. 3. Schematic of the Guidant 27-mm TiNi-encapsulated ^{32}P intravascular brachytherapy sources. The chemical and physical composition of the internal ^{32}P source material is proprietary and cannot be disclosed.

to a NIST ^{32}P solution standard (within a 5-ml glass ampoule) which was used in the absence of a ^{32}P standard in a more suitable geometry. This calibration was not expected, a priori, to necessarily be very reliable because the instrument's response must be very different for the resulting bremsstrahlung spectra from these two very different source geometries. The second calibration was obtained by LS measurements on a very aged seed that had been placed directly into an LS cocktail for counting. Such measurements could not be performed until the source had sufficiently decayed to a level that was within a counting-rate range that could be handled by the LS spectrometer (less than a few thousand counts per second). The ^{32}P activity of this aged source, which was used to determine a new calibration factor for the well counter, was then obtained from calculations of the ^{32}P β spectrum that exited the source's TiNi jacket, from estimates of the overall LS detection efficiency for these degraded β particles and from a huge ^{32}P decay correction. Activity measurements of the sources as obtained with these two preliminary calibrations were noted to result in differences of approximately 30%. Neither calibration was initially considered to be more reliable than the other.

2.2. On the protocol for the chemical digestion, and the basis for the radionuclidic assay

The overall protocol for the chemical digestion and radionuclidic assay is outlined in the schematic of Fig. 4. In general terms, the scheme may be viewed as consisting of the following sequential steps: (i) following all earlier non-destructive measurements (e.g. dosimetry, photonic-emission-spectrometry impurity analyses and relative ionization-chamber-based activity assessments), the 'active' portion of the long TiNi wire was cut off; (ii) the seed's jacket was dissolved to expose the internal ^{32}P-containing source material; (iii) the ^{32}P activity was extracted from the source material by repetitive solution transfers to a master solution; (iv) the master solution was appropriately diluted and assayed by LS spectrometry and (v) the residual activity in the remaining part of the extracted source material, along with the apparatus used to effect the solution transfers, was also assayed by LS spectrometry and was used to correct the master solution assay. A similar set of steps were performed on the adjacent section of the TiNi wire.

The nature of the internal source material precluded finding any single solvent that could completely digest the entire seed while ensuring the quantitative retention of ^{32}P in solution. The task would have been decidedly easier had such a 'magic' solvent existed! The reasoning for the ultimately-chosen digestive solvents may prove to be instructive. The relevant questions, of course, involved: how should one dissolve the seed's TiNi jacket?; how should one extract the activity from the internal source which contained a nearly chemically-impervious component?; what will be the fate of the extracted activity during these chemical treatments? and how does one insure that the process will be quantitative in accounting for all of the activity contained in the seed? Additional concerns were that any resulting diluted solution had to be stable for the extracted

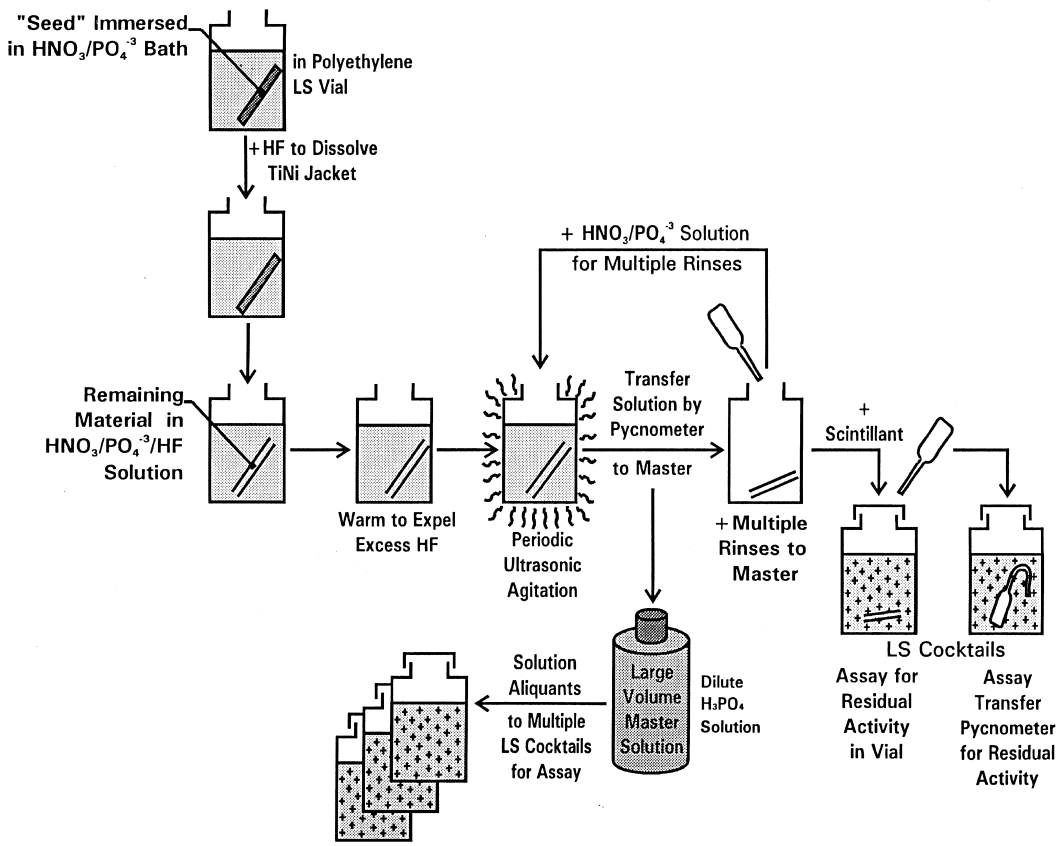

Fig. 4. Illustration of the overall protocol used for the chemical digestion and radionuclidic assay of Guidant ^{32}P brachytherapy sources.

^{32}P and that this solution had to be compatible in forming adequate LS cocktails.

The answer to the first question presented an immediate dilemma. Titanium steels and alloys retain almost all of the dissolution properties of Ti metal itself (Landis and Kaye, 1971). It is very resistive and largely unreactive to all common alkalies, mineral acids (except HF), gases, salts and even liquid metals. It initially reacts with most non-oxidizing acids (HCl, H_2SO_4, etc.), but then often forms an insoluble oxide layer of TiO_2 that prohibits further dissolution (Barksdale, 1953). Even the use of strong oxidizing acids (like concentrated hot HNO_3 or HCl–HNO_3 aqua regia) tends to form an oxide layer and fails to dissolve the metal. Any Ti alloy in bulk may therefore not dissolve in most oxidizing or non-oxidizing acids (except HF) or even in combination (like aqua regia) under usual conditions. Titanium alloys, like TiNi, in non-bulk form may dissolve in non-oxidizing acids like HCl, but the usual way is under vigorous boiling (and agitation) in a reflux condenser and over very long time intervals. For example, it has been reported (Landis and Kaye, 1971) that a 100-mg sample of pulverized Ti steel in 200 ml of 6 mol l^{-1} HCl required over 90 h of vigorous boiling to achieve dissolution (and about 0.2% of the sample remained as undissolved solids). It may also be noted that any type of reflux-condenser arrangement would also require more than heroic efforts to keep the seed-dissolution process quantitative on a radiochemical basis. Titanium and its alloys can however be readily dissolved in HF, which is about the only non-oxidizing acid that is known to always reliably work. Exceptions to this include more exotic stuff like HBF_4 and other fluoroboric acids (Barksdale, 1953). The dilemma occurs because use of HF (or any other non-oxidizing acid like HCl or H_2SO_4) can create serious problems for the retention of ^{32}P since their use may result in the formation and release of the volatile and exceedingly poisonous, phosphine (PH_3) gas (Cotton and Wilkinson, 1966). In fact, phosphorus is often separated from solutions by the use of HCl to form PH_3, which is removed by sweeping with an inert gas stream like Ar (Landis and Kaye, 1971). Stable ^{32}P solutions require an oxidizing medium (like HNO_3), which, as noted, is unlikely to dissolve the TiNi alloy, and an excess of PO_4^{-3} ions. In

short, HF (as a non-oxidizing acid) is best for dissolving TiNi, but worst for possible ^{32}P losses.

Let's now consider the next questions, which are concerned with the internal source-material portion of the seed. Based on its known composition, it was evident that a principal physical part of its internal structure was not likely to be dissolved by any usual solvent. At least not any inorganic solvent or any organic solvent that would possibly survive in the presence of the acid needed to dissolve the TiNi jacket. Yet, it seemed likely that the ^{32}P activity in its known chemical and physical form might be adequately extracted from this physical, chemically-impervious part by exchange with a HNO_3 solution. Furthermore, it seemed that if the seed were immersed in a HNO_3 bath prior to the addition of HF to dissolve the TiNi jacket, then one could lessen (or obviate) any loss of activity by using a large excess of PO_4^{-3} ions in the HNO_3 bath.

Further reflection on the remaining questions as to how to insure that the procedure was quantitative lead directly to the scheme laid out in Fig. 4, which was designed to utilize a minimum of solution vessels and transfer tools (all of which could be subsequently examined for residual activity). Ultimately, to verify the quantitative retention of ^{32}P by this scheme, radiochemical tracing experiments were performed on each of the individual operations shown in Fig. 4.

The adopted method then consisted of initially immersing the cut-off seed in a small-volume (nominal 5 to 10 ml) bath of a dilute 1.5 mol l^{-1} HNO_3 solution which had a large excess of inactive PO_4^{3-} carrier ions (240 to 400 μg PO_4^{3-} per g of solution). The bath and seed were contained inside a conventional 22-ml, high-density polyethylene LS vial (which was used for later, direct evaluations of any residual activity). The TiNi jacket was subsequently dissolved by adding a few tenth's of a ml of concentrated HF (nominal 30 mol l^{-1}) to the bath. As noted, dissolution of the TiNi required the use of HF, but could not be directly used because of the possibility of losing ^{32}P by the formation and release of PH_3. Hence, the HNO_3/PO_4^{3-} bath was used to insure retention of the ^{32}P in solution. The TiNi dissolution in the HNO_3/PO_4^{3-}/HF bath was usually complete within 6 or more hours. In several trials, the resulting solution (containing the dissolved jacket) initially appeared to have traces of an insoluble black-flaky particulate matter that had been previously observed to have formed on the surface of the TiNi during the dissolution process. These undissolved solids invariably disappeared after the passage of another 12 to 24 h, particularly if heat was applied. Excess HF was removed in some trials by gentle heating (less than 70°C) over the course of another several hours. The removal of excess HF was done only in those cases where very small dilutions of the master solution were made. Even traces of HF in LS cocktails are known to have very deleterious effects on the performance of commercially-available scintillation fluids (scintillants).

Following the TiNi-jacket dissolution and possible removal of excess HF, the ^{32}P that was still contained in the residual source material was brought into solution by exchange with the HNO_3/PO_4^{3-} bath. This step was effected by a repetitive sequence of carefully-executed quantitative solution transfers and rinses (using an aspirating polyethylene pycnometer) that were typically performed over the course of many days. After each of these transfers, the bath was replenished with fresh HNO_3/PO_4^{3-} carrier solution. Periodic ultrasonic agitation over these periods was employed to accelerate the exchange. The ultrasonic agitation was used very intermittently, and lasted for only periods of 1 or 2 h to avoid excessive ultrasonic heating of the bath. Typically, several such short agitations (followed by bath cooling periods) were performed between each solution transfer and rinse. The effectiveness of the exchange removal of ^{32}P during these operations was highly dependent on the internal composition of the source materials, and was logically consistent with the known, but varying composition of each of the four sources. The variations were dramatic in the sense that nearly complete removal of the ^{32}P was achieved in one of the sources (#5) over only a three-day digestion period, whereas source P-97-15-2 required over a 50-day effort. Many of these timing details are summarized in Table 1. The progress of the exchange removal was monitored in all cases by making relative bremsstrahlung-emission measurements of the bath (after replenishments) with a thin-windowed NaI(Tl) ratemeter. Fig. 5 demonstrates the temporally-dependent removal of the activity from one of the more easily extractable seeds (P-96-32-3) as obtained from these relative measurements.

All of the transfers and rinses from these steps were added to a relatively large-volume (nominally from less than 100 up to 2000 ml), very dilute 0.005 to 0.01 mol l^{-1} H_3PO_4 master solution whose total diluted mass was gravimetrically determined. This solution was then assayed by efficiency-tracing LS spectrometry (see Section 2.3).

Any residual activity in the remaining solid portion of the source material was also evaluated by LS spectrometry. This was effected by adding scintillant to the original LS vial (in which all of the previous operations were performed) and counting it to perform the assay. Similarly, the solution transfer and rinse tools were also evaluated. In this case, the sole solution-transfer instrument (the transfer pycnometer) was filled with the scintillation fluid and placed inside another LS vial. This second LS vial was one that had been used as an intermediate vessel that held the carrier sol-

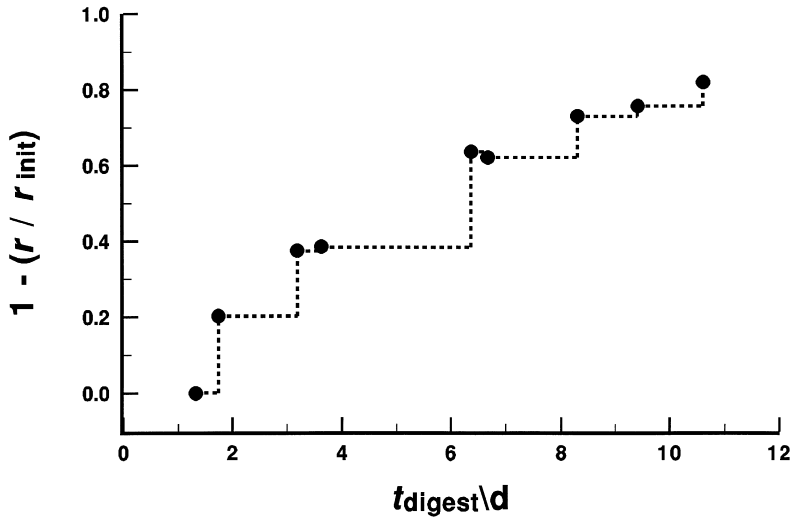

Fig. 5. Normalized results of relative bremsstrahlung-emission measurements for seed P-96-32-3 (as obtained with a NaI(Tl) rate-meter) after sequential bath replenishments (following each solution transfer). Values of the so-called 'exposure rate' r were normalized to the initial reading r_{init} to give a removal fraction $(1 - r/r_{\text{init}})$ as a function of the digestion time t_{digest} (in units of days). The curve illustrates typical data that was used to monitor the extraction of activity out of the residual source material. Neither the number and duration of ultrasonic agitations, nor the number of solution transfers and rinses between each reading were constant.

ution for filling the pycnometer for replenishment of the bath. Additional scintillant was then added to fill the vial and this vial was also assayed. This approach of directly assaying all of the component parts and tools, of necessity, could account for the total ^{32}P activity originally contained in the original cut-off seed.

Using a virtually identical sequence of steps, various cut-off lengths of the originally submitted sources adjacent to the active seed portions (see Table 1) were also digested and assayed for any contained activity.

2.3. On the LS efficiency-tracing methodology

The resultant large-volume master solution and various residual-activity vials were then assayed for ^{32}P and ^{33}P by an efficiency-tracing 4πβ LS spectrometric method that is somewhat routine for this laboratory (Collé, 1997a). It is based on well-established procedures for the assay of gravimetrically-determined aliquots of solutions containing β-emitting radionuclides (Collé and Zimmerman, 1996a,b, 1997; Collé, 1997b, 1998; Zimmerman and Collé, 1997a,b,c).

For a given LS cocktail formed with an aliquant of mass m of a ^{33}P/^{32}P solution in some suitable scintillant, the total number of counts C_i detected in a counting interval T can be given by

$$C_i/mT = A_{32(0)}\epsilon_{32}\exp(-\lambda_{32}t_i) + A_{33(0)}\epsilon_{33}\exp(-\lambda_{33}t_i) + B_i/T \quad (1)$$

where $A_{32(0)}$ and $A_{33(0)}$ are the *massic* activities of ^{32}P and ^{33}P in solution (activity per unit mass of solution) at some $t_i = 0$ reference time, respectively; ϵ_{32} and ϵ_{33} are the respective 4πβ LS detection efficiencies (at time t_i if they are temporally dependent); λ_{32} and λ_{33} are the ^{32}P and ^{33}P decay constants, respectively, and B_i/T is the estimation of the background counting rate for a composition-matched blank cocktail at time t_i. The symbolic notation used here follows that given in the more detailed treatment of Collé (1997a). In the assay of the residual-activity vials, the mass m is irrelevant and $A_{32(0)}$ and $A_{33(0)}$ in Eq. (1) then represent the *total* activities in the vials. The counting intervals T are always $1/\lambda_{32} \gg T \ll 1/\lambda_{33}$. The ϵ_{32} and ϵ_{33} efficiencies are evaluated by efficiency tracing with composition-matched ^{3}H-standard cocktails using the CIEMAT/NIST methodology (outlined below). Therefore, the background-corrected counting rate $R_i = (C_i - B_i)/mT$ at time t_i at the midpoint of the counting interval T is just

$$R_i = A_{32(0)}\epsilon_{32}\exp(-\lambda_{32}t_i) + A_{33(0)}\epsilon_{33}\exp(-\lambda_{33}t_i) \quad (2)$$

which is easily transformed into a linear form:

$$Y = A_{32(0)} + XA_{33(0)} \quad (3)$$

with $Y = R_i/\epsilon_{32}\exp(-\lambda_{32}t_i)$ and $X = [\epsilon_{33}\exp(-\lambda_{33}t_i)]/[\epsilon_{32}\exp(-\lambda_{32}t_i)]$. With sufficient (R_i, t_i) counting data pairs, $A_{32(0)}$ and $A_{33(0)}$ could be obtained as constant parameters by fitting the (R_i, t_i) data to the functional form of Eq. (2). The linearized equation (Eq. (3)), in which the intercept of Y at $X = 0$ is equal to the ^{32}P

activity $A_{32(0)}$ and the slope dY/dX is equal to the ^{33}P activity $A_{33(0)}$, was used as a powerful graphical tool for examining the quality of the input (R_i, t_i) measurement data and the quality of the resolution (Collé, 1997a).

The acronym CIEMAT/NIST refers to the two laboratories that collaborated in developing the employed LS spectrometry tracing methodology, viz. the Centro de Investigaciones Energeticas, Medioambientales y Technologicas (CIEMAT) and NIST. Features of the method have been described in numerous publications by the CIEMAT/NIST originators (Grau Malonda and Garcia-Torano, 1982; Coursey et al., 1985, 1986, 1989, 1991). The references that follow are given to direct the reader to some of the method's most important aspects as employed for this work. Specific details on the method's practical application, as it is presently invoked in this laboratory, are given by Collé and Zimmerman (1996a,b, 1997) and Zimmerman and Collé (1997a,b,c). They (Collé and Zimmerman, 1996b, 1997) have also nicely summarized and given an overview of the calculational protocol. This protocol employs various updated and revised versions of the CIEMAT-developed EFFY code (Garcia-Torano and Grau Malonda, 1985; Grau Malonda et al., 1985; Garcia-Torano, 1993) to determine the detection efficiencies for cocktails of the traced radionuclide (under known and varying quench conditions) by following the experimentally-determined efficiencies for closely-matched cocktails of ^{3}H. Tritium (^{3}H) is recommended to serve as the matched (in terms of cocktail composition and quenching) standard since extrapolations to the lower-energy portions of the β spectra are more sensitive than that obtained with higher-energy β-emitting standards like ^{14}C (Coursey et al., 1986, 1989). The importance of cocktail matching between the standard cocktails and those of the traced radionuclide has been treated by Collé (1997c). Similarly, the need to understand the cocktail-composition systematics, such as the effects of the aqueous mass fraction (Collé and Zimmerman, 1996a,b) or ionic loading (as it affects cocktail stability and what has been termed cocktail 'tractability'), is critical (Collé, 1998). Zimmerman and Collé (1997a), Collé (1997c) and Collé and Zimmerman (1997) have also identified and addressed some of the critical underlying assumptions regarding the method's applicability. They too (Collé and Zimmerman, 1996b) have developed and presented a detailed uncertainty model for the CIEMAT/NIST method's measurement process.

2.4. On the LS cocktail preparations, LS spectrometers and measurements

The routine gravimetric, source-preparation procedures used in our laboratory as they apply to the preparation of LS counting sources (such as those prepared for this work), as well as estimations of their associated uncertainties, have been treated at length previously (Collé, 1995; Collé et al., 1995; Collé and Kishore, 1997). Mass determinations for the aliquants have relative standard uncertainties of about $\pm 0.05\%$ (refer to Taylor and Kuyatt (1994) for internationally-accepted definitions of the uncertainty terms). The LS counting sources were prepared in all cases with a diisopropylnapthalene (DIPN)-based, 'ready-to-use', commercially-prepared scintillant (namely, 'Ultima Gold AB' (Packard Instrument Co., Meriden, CT)) and were contained in 22-ml, high-density polyethylene vials with polymerized-urea screw caps. The total cocktail mass was always kept constant at 10 g to within about 0.01 g (refer to Zimmerman and Collé, 1997c) for cocktail volume (mass) effects).

The ^{3}H-standard cocktails used for the ^{32}P and ^{33}P efficiency tracing were prepared with aliquants of carefully-prepared gravimetric dilutions of a NIST ^{3}H (tritiated-water) standard (NIST, 1991). Efficiency variations for the tracing were achieved by either using varying aliquant sizes (and hence variable aqueous mass fraction and quenching) or by the use of a 10% solution of CH_3NO_2 in ethanol as an imposed quenching agent. The ^{3}H cocktails were in all cases composition matched to the $^{33}P/^{32}P$ cocktails by the addition of proportionate amounts of the blank carrier solutions that were used to prepare the $^{33}P/^{32}P$ master solution.

Measurements on the prepared cocktails were mainly performed with one of our two LS spectrometers, namely the NIST 'system B'. A few measurements were also performed with our 'system P'. The principal operating characteristics of the two spectrometers have been outlined previously (Collé and Kishore, 1997; Collé and Zimmerman, 1997). Descriptions of these operating characteristics, their respective performance and use within this laboratory for various radionuclidic calibrations are available (Collé, 1993, 1995, 1997b; Collé and Thomas, 1993; Collé et al., 1995; Collé and Zimmerman, 1996b, 1997; Collé and Kishore, 1997). Use of the two spectrometers on the identical set of cocktails provides the benefit of being able to verify that the efficiency tracing (and hence the accuracy of the assay) is indeed instrument independent. The two instruments have some similar and some substantially different operating characteristics and have decidedly different detection thresholds (refer particularly to Collé et al. (1994)).

The quench indicating parameter (QIP) used to account for small quenching differences between the matched ^{3}H-standard and $^{33}P/^{32}P$ cocktails was an instrument-derived Horrocks number H for the 'system B' spectrometer and a 'transformed spectral index of the external standard' (tSIE) for 'system P'. The calcu-

lated QIP-adjusted ^{32}P and ^{33}P efficiencies, ϵ_{32} and ϵ_{33}, as obtained from tracing with the experimentally-determined ^{3}H efficiencies were obtained with the EFFY4 code (Garcia-Torano, 1993). Table 1 includes the nuclear data (ENSDF, 1997) for the $E_{\beta(max)}$ values that were as input for the EFFY4-code calculations, as well as the half-lifes that were used for decay corrections. Fig. 6 shows the slight dependence of the ϵ_{32} and ϵ_{33} efficiencies as a function of the ^{3}H efficiency.

Each master-solution assay typically used more than one set of prepared cocktails which were measured over periods of weeks (see Table 1) to adequately resolve the ^{33}P and ^{32}P components. Typical LS measurement data and the analyses for these assays has been presented in Collé (1997a). This paper, in its first example, actually contains a tabular summary of the experimental conditions for the assay of the master solution that was obtained from the digestion of seed P-96-32-3. It includes complete specifications on: the number of cocktails used; the cocktail masses, solution aliquant sizes and aqueous mass fractions; the imposed quenching agent (to vary efficiencies); the efficiency ranges for ^{3}H, ^{32}P and ^{33}P; the number of measurements on each cocktail; the cocktail 'ages' at the measurement times; the counting-time intervals and the time intervals over which the measurements were made. The conditions are very representative of those used for the assays of the other three seeds.

Assay of the residual activity vials were based on relative LS counting rate measurements (with comparisons made to cocktails prepared with the master solution) with corrections for efficiency differences. The LS detection efficiencies for these vials were estimated from ^{3}H efficiencies obtained with comparably-prepared ^{3}H-spiked blanks.

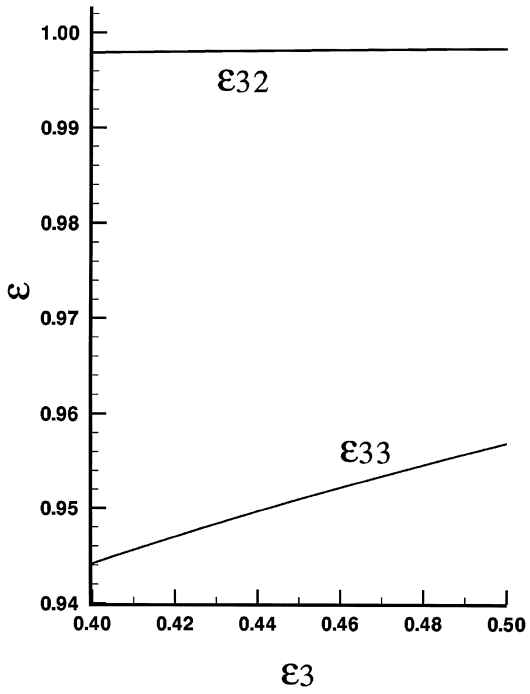

Fig. 6. EFFY4-code calculations for the ^{32}P and ^{33}P LS detection efficiencies (ϵ_{32} and ϵ_{33}) as a function of that for ^{3}H over the range of typical experimental ^{3}H efficiencies: $0.40 \leq \epsilon_3 \leq 0.50$.

Table 2
Results of the tracing experiments to evaluate possible losses in the chemical digestion procedure. The fractional recovery is defined as $Q = A_{after}/A_{before}$ (see text). The cited uncertainty intervals correspond to standard uncertainties propagated from the LS measurement precision and the uncertainties in the gravimetrically-determined mass normalizations

Experimental conditions for the procedural step tested	Fractional recovery, Q		
	trial 1	trial 2	trial 3
Immerse seed in HNO_3/PO_4^{3-} bath; add HF to dissolve TiNi jacket; after 4 to 6 h	0.9984 ± 0.0029	1.0013 ± 0.0038	–
Residual source material in HNO_3/PO_4^{3-}/HF bath (TiNi jacket dissolved); after 18 to 45 h	1.0006 ± 0.0034	0.9989 ± 0.0030	1.0016 ± 0.0022
Heat uncovered bath in vial to 72 ± 3°C for 5 h to remove excess HF	1.0009 ± 0.0032	0.9980 ± 0.0053	–
Transfer bath solution from vial with three rinses	0.9974 ± 0.0031	–	–
Ultrasonic agitation (with attendant warming) of HNO_3/PO_4^{3-} bath for 1.2 to 3.7 h	0.9985 ± 0.0053	1.0030 ± 0.0035	–
Eight repetitive solution transfers (about twice per day) over six days	0.9978 ± 0.0045	–	–
Repetitive ultrasonic agitations (two or three times per day) over four to five days with intermediate solution transfers and rinses	0.9981 ± 0.0035	0.9986 ± 0.0056	0.9978 ± 0.0033

2.5. On the radiochemical tracing experiments used to evaluate the digestion procedure

Each of the individual steps of the chemical procedure (outlined in Fig. 4) was independently evaluated for possible ^{32}P losses by radiochemical tracing experiments. One or more trials were conducted for each step listed in Table 2. The fractional recovery Q was defined as $Q = A_{after}/A_{before}$ where A_{before} is the initial activity in a test vial at the starting conditions of the step to be evaluated and where A_{after} is the total activity remaining in the vial after the procedural step was performed. The ratio of these activities could in turn be related to mass-normalized relative LS counting rate measurements on LS cocktails that contained aliquants of A_{after} and A_{before}.

Two slightly varying approaches were used. In both cases, test vials were prepared with solutions and blank source materials that simulated the step's starting conditions. Using a $^{32}P/^{33}P$ solution that had an equivalent *massic* activity C (with an arbitrary $^{33}P/^{32}P$ impurity ratio I), the test vials (having a total solution mass M) were spiked with aliquants of mass m_{add} so that the initial activity in the vial was $A_{before} = Cm_{add}$ with a *massic* activity of $A_{before}/(M + m_{add}) = Cm_{add}/(M + m_{add})$. At the conclusion of the step's procedure, multiple aliquants of mass m_a were taken from the test vial and added to LS cocktails for counting. To evaluate C on a relative basis in terms of A_{before}, another set of composition-matched LS reference cocktails were prepared using aliquants of mass m_{ref} from the $^{32}P/^{33}P$ spiking solution. The background-corrected LS rates for the two sets are: $R_{after} = A_{after}\epsilon[m_a/(M + m_{add})]$ and $R_{ref} = C\epsilon m_{ref}$ where ϵ is a common LS detection efficiency for the reasonably-matched cocktails. With $C = R_{ref}/\epsilon m_{ref}$, it follows that $A_{before} = R_{ref}m_{add}/\epsilon m_{ref}$ and

$$Q = (R_{after}/R_{ref})[(M + m_{add})/m_a](m_{ref}/m_{add}). \quad (4)$$

In the second approach, A_{before} was evaluated differently by taking multiple aliquants of mass m_b from the spiked test vial (prior to the procedural step) to form yet another set of LS cocktails. In this case, the LS rates are $R_{before} = A_{before}\epsilon m_b/(M + m_{add})$ and $R_{after} = A_{after}\epsilon m_a/(M + m_{add} - m_{out})$ where m_{out} is the total mass of solution extracted (for the m_b aliquants) from the starting $(M + m_{add})$ solution. In this second case, Q was obtained from

$$Q = (R_{after}/R_{before})(m_b/m_a)[(M + m_{add} - m_{out})/(M + m_{add})]. \quad (5)$$

In both approaches, the two sets of cocktails (typically three to five of each) were interspersed for counting over relatively short time intervals ($T \leq 20$ min) so that the LS counting rate ratios R_{after}/R_{ref} or R_{after}/R_{before} were largely independent of the impurity ratio I in the spiking solution. This conditional (of having each R_{after} measurement bracketed between measurements of R_{ref} or R_{before}, and vice versa, over short time intervals) obviated the need for knowing (or determining) I and the need for performing two-component decay corrections.

3. Results and discussion

3.1. On the evaluation of possible ^{32}P losses in the chemical digestion procedure

The results of the radiochemical tracing experiments which were used to validate the quantitative retention of ^{32}P during the chemical digestion procedure are summarized in Table 2. All of the trial 1 results for each tested step were derived from the Eq. (4) approach, while those for trials 2 and 3 were obtained from the Eq. (5) approach.

The fractional recovery Q in every case is wholly consistent with virtually no losses (i.e., $Q = 1$) within the measurement uncertainties for the tracing experiment. The cited standard uncertainties in Q, derived from the replication precision in determining either R_{after}/R_{ref} or R_{after}/R_{before} and estimates for the uncertainty in the gravimetrically-determined mass normalizations, largely reflect the inherent within-sample and between-sample variations in the LS measurements that were used for these recovery experiments.

These findings not only verified the quantitative nature of the devised digestion procedure, but could also be used to establish realistic uncertainty estimates for possible activity losses during the chemical digestion and solution transfers. These estimates were used in the uncertainty assessment for the assay results (Section 3.3).

3.2. On the LS spectrometry of intact, aged seeds

The very-aged, 3-mm seed #5 (see Table 1) was examined directly by LS spectrometry (in its intact form) prior to its digestion. This was done largely out of mere intellectual curiosity and insofar as it served as the basis for one of the preliminary Guidant calibrations (see above).

For this examination, the seed was immersed into the scintillant and supported in a vertical, upright position in the near center of the LS vial using a loosely-wound, nichrome-wire stanchion. Neither the LS spectral shape nor the counting rate was found to be position sensitive. Relative LS counting rates for the seed inside the stanchion and lying at the bottom of the LS vial differed by less than 0.04%.

Despite the source's large ^{33}P internal content at the time of measurement, the resultant LS spectrum for the intact TiNi-encapsulated seed appeared to be that for a pure ^{32}P spectrum. The spectrum, shown in Fig. 7(a), was obtained with the 'system B' spectrometer which has logarithmic pulse amplification so that the difference between any two channels (c_2-c_1) is proportional to the logarithmic energy ratio $\log(E_2/E_1)$. The contrast with the spectrum obtained with this seed's master solution (following the digestion) is dramatic. As seen in Fig. 7(b), the large ^{33}P content in the solution is evident. Based on the LS decay data and resolution of the $A_{32(0)}$ and $A_{33(0)}$ components (from Eq. (2)), the impurity ratio at the reference time was $I = 7.2 \pm 0.2$, that is over seven times more ^{33}P than ^{32}P. This very large ^{33}P content allowed a direct determination of the relative ^{33}P and ^{32}P activity components by spectral stripping procedures, whose results comported reasonably well (within $\pm 6\%$) with that obtained from the resolved decay data.

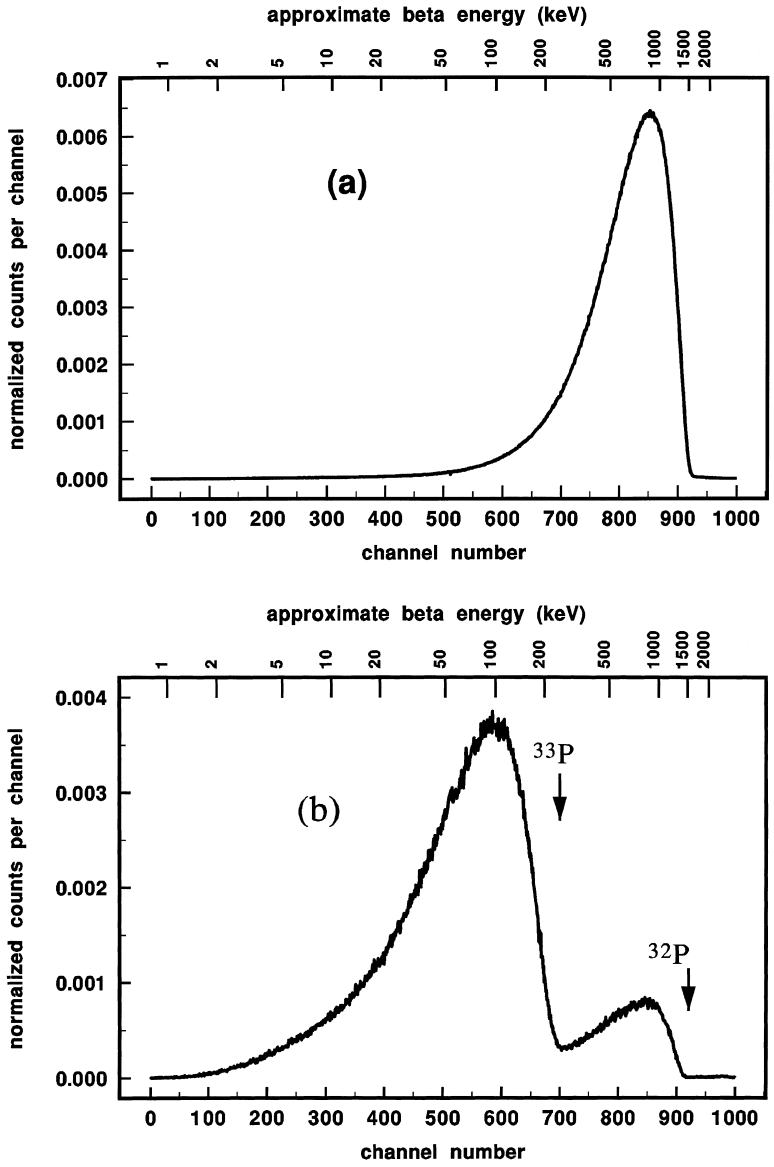

Fig. 7. Experimental LS spectra obtained with the NIST 'system B' spectrometer for (a) the aged, intact TiNi-encapsulated seed #5 and (b) for the master solution obtained from the chemical digestion of seed #5. Both spectra have been normalized so that their integral areas equal unity. Refer to the text for discussion.

The effective LS detection efficiency ϵ_{LS} for the intact seed, obtained from the ratio of the apparent, background-corrected, LS counting rate R_{LS} and the assayed ^{32}P activity A_{32} (decay corrected to the R_{LS} measurement time), was $\epsilon_{LS} = R_{LS}/A_{32} = 0.94 \pm 0.08$. This high efficiency was a very surprising finding since there was no evidence to suggest that any of the ^{33}P β particles escaped from the TiNi seed, and since this value was substantially greater than the number of ^{32}P β particles that could possibly emerge from the TiNi jacket. Calculations by Seltzer (1997) confirmed that less than 0.1% of the ^{33}P β particles and approximately 70% of those from the decay of ^{32}P exited the source. Fig. 8 compares a ^{32}P β spectrum to the results of Seltzer's calculation for the spectrum exiting from a 27-mm seed TiNi seed. Calculational results for a 3-mm seed were essentially identical. Even calculations of the production and emission of secondary electrons (produced by stopped β particles in the TiNi) cannot account for an efficiency as high as $\epsilon_{LS} = 0.9$. The only plausible explanation is that a substantial fraction of the low-energy-bremsstrahlung photons (which are not coincident with any emitted β particles that escape the seed) are also being detected.

This unexpected ϵ_{LS} finding may account for the apparent overestimation by Guidant for their reported ^{32}P activities, which were derived by a preliminary calibration based on this LS-measurement approach.

3.3. On the ^{32}P and ^{33}P-impurity radionuclidic assay results

Table 3 contains the results for the ^{32}P and ^{33}P activities in the four seeds, at their respective reference times, as certified by NIST. The results were primarily derived from assays of the master solutions for the digested seeds, but also included corrections for the fraction of activity in the undigested portion of the seed and for the fraction of residual activity in the transfer tools. As noted in Table 3, the uncertainties in both the ^{32}P and ^{33}P-impurity activities were considerably variable and were highly dependent on the impurity ratios at the assay times and on the residual activity fractions. These issues will be addressed more fully in Sections 3.4 and 3.5.

3.4. On other radionuclidic impurities

Impurity analyses for possible photon-emitting impurities were performed on the originally-submitted, undigested seeds P-96-32-3 and P-97-23-6 by high resolution γ-ray spectrometry using high-purity germanium (HPGe) detectors.

The first of these seeds was extensively examined over nearly a nine-day period and was found to have an ^{124}Sb impurity of 19.3 ± 4.9 Bq as of a NIST Report of Test reference time of 1200 EST 1 November 1996, which corresponded to an $^{124}Sb/^{32}P$ impurity ratio of $(6.1 \pm 1.5)10^{-7}$. Decay corrections to the earliest known Guidant reference time (which presumably was near the source preparation time) yielded

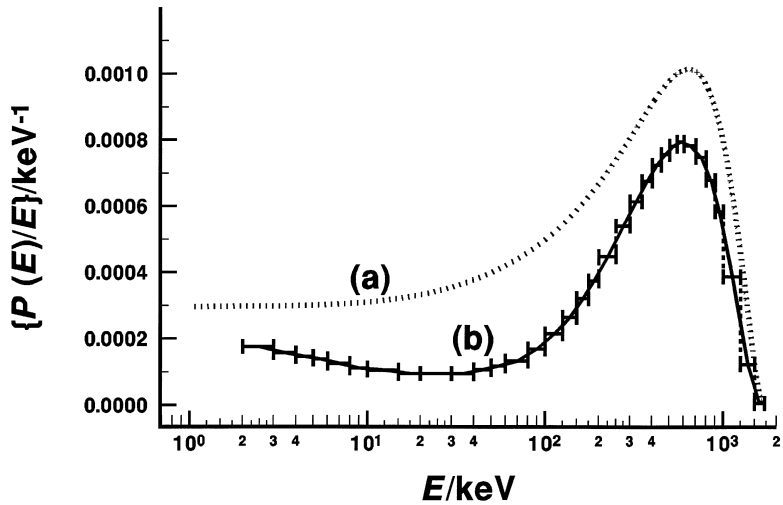

Fig. 8. Theoretical energy spectra (a) of β particles from ^{32}P decay, normalized to $\int [P(E)/E]\,dE = 1$; and (b) of laterally-escaping electrons from a 27-mm TiNi-encapsulated ^{32}P seed, normalized to one β particle. The former spectrum (a) was obtained by calculations with the EFFY4 code; the latter (b) was the result of calculations by Seltzer (1997). The horizontal bars in spectrum (b) are the energy-bin widths used for the Monte Carlo calculations.

Table 3
Assay results for ^{32}P and ^{33}P on the four submitted sources

Source identification	#5	P-96-32-3[a]	P-97-15-2	P-97-23-6
Reference time[b]	**1200 EST 1 December 1996**	**1200 EST 14 January 1997**	**1200 EST 22 August 1997**	**1200 EST 6 October 1997**
Phosphorus-32 activity	**1.004 kBq**	**874.5 kBq**	**1.211 MBq**	**14.15 MBq**
Expanded uncertainty on ^{32}P activity[c]	**0.078 kBq**	**8.4 kBq**	**0.047 MBq**	**0.20 MBq**
Phosphorus-33 activity	**7.215 kBq**	**150.4 kBq**	**0.5003 MBq**	**1.567 Mbq**
Expanded uncertainty on ^{33}P activity[c]	**0.121 kBq**	**6.5 kBq**	**0.0187 MBq**	**0.121 MBq**
$^{33}P/^{32}P$ activity ratio	**7.186**	**0.1720**	**0.4131**	**0.1107**
Expanded uncertainty on $^{33}P/^{32}P$ activity ratio[d]	**0.219**	**0.0080**	**0.0183**	**0.0085**
Fraction of total activity in adjacent TiNi section[e]	section not available	$\simeq 2\cdot10^{-4}$[f]	$(6 \pm 2)10^{-7}$	$(8 \pm 3)10^{-8}$
Fraction of total residual activity (unrecovered from digestion and dilution) in seed[e]	0.0017 ± 0.0001	0.0021 ± 0.0003	0.075 ± 0.009	0.0090 ± 0.0053[g]
Fraction of total residual activity on tools[e]	not detectable[f]	$\simeq 3\cdot10^{-5}$[f]	$(1.5 \pm 0.3)10^{-5}$[h]	$(1.5 \pm 0.2)10^{-4}$

Values certified by NIST are in bold-face type.[a]The values reported here differ from those given on a previous NIST Report of Test (NIST, 1997) because of decay corrections to the reference time for the dosimetry measurements.[b]The reference times given here are those for the LS measurements and regression.[c]For a coverage factor of $k = 2$ which is assumed to correspond to an uncertainty interval at a 95% confidence level (see Tables 4 and 5).[d]For a coverage factor of $k = 2$. The uncertainty in the $^{33}P/^{32}P$ activity ratio can not be directly propagated from the uncertainties in the ^{32}P and ^{33}P activities because of measurement correlations (see Table 6).[e]The given uncertainty intervals are that for a $k = 2$ coverage factor.[f] Efforts were not made to determine this value more precisely, and may be considered to be an upper bound.[g]This value could have been determined more precisely (at later times) with additional measurements after subsequent decay of the residual source to lower LS counting rates.[h]This value may be underestimated since the established procedure was modified during the chemical digestion. Additional handling tools were employed to extract and cut the solid portion of the seed into four pieces while it was contained in the dissolution vessel.

an 'initial' impurity ratio of $6\cdot10^{-8}$. Collé (1997a,b,c) recently noted that most commercial sources of ^{32}P, in addition to the ^{33}P impurity, often contains ^{124}Sb. Its origin is inexplicable considering the likely irradiation mechanisms and target materials used to prepare the ^{32}P sources. The $^{124}Sb/^{32}P$ impurity ratio is generally in the range of 10^{-6} to 10^{-8} for freshly-prepared ^{32}P supplies. Based on over a decade of γ-ray spectrometry results from this laboratory (Schima, 1996) with many different commercial source of ^{32}P, it has been observed that ^{124}Sb is not only almost always detected, but it is largely the only γ-emitting impurity ever observed.

A more cursory examination of seed P-97-23-6 failed to detect any γ-ray emitting impurities.

The energy-dependent upper limits for any other unobserved γ-rays in either seed were:

$< 8\cdot10^{-5}$ γ s^{-1} per Bq of ^{32}P
for energies 12 keV $\leq E_\gamma \leq$ 88 keV,
$< 4\cdot10^{-5}$ γ s^{-1} per Bq of ^{32}P
for 96 keV $\leq E_\gamma \leq$ 507 keV,
$< 2\cdot10^{-6}$ γ s^{-1} per Bq of ^{32}P
for 515 keV $\leq E_\gamma \leq$ 1456 keV,
$< 6\cdot10^{-6}$ γ s^{-1} per Bq of ^{32}P
for energies 1465 keV $\leq E_\gamma \leq$ 2250 keV,

at the reference times for the ^{32}P activities given in Table 3.

From the time-dependent LS data which was used to resolve the ^{32}P and ^{33}P activity components (typically accumulated over many weeks), there was no evidence to suspect the presence of any other pure β-emitting impurity. Upper limits for any such impurity could be established from the quality of the ^{32}P and ^{33}P fitted resolutions. These upper limits range from $< 0.2\%$ for seed P-96-32-3, to $< 0.04\%$ for P-97-15-2, to $< 0.1\%$ for seed P-97-23-6 where the percentages are with respect to the ^{32}P activity at the start time of the LS measurements as given in Table 1. For purposes of these calculations, it was assumed that the hypothetical, unobserved, pure β-emitting impurity had a LS detection efficiency of 0.7 and that it had a half-life $T_{1/2}$ in the range 10 d $< T_{1/2} <$ 400 d.

3.5. On the residual activity determinations

Determinations of the fraction f_{res} of the ^{32}P and ^{33}P activity that was not extracted, and that remained unrecovered in the remaining portion of the digested seed, were the most difficult measurements that had to be performed. Firstly, in order to perform the LS measurements on these remaining portions, the activity content had to be low enough for the LS counting rate to be within a range that could be handled by the spec-

trometer without either paralyzing the pulse electronics or introducing impossible-to-correct deadtime errors. One could, alternatively, delay the LS measurements until the activity in the remaining portion decayed to sufficiently low levels. Secondly, the LS detection efficiencies for the ^{32}P and ^{33}P activities in the remaining portion had to be estimated. The efficiencies undoubtedly had to dwell somewhere between those for ^{32}P and ^{33}P in solution (Fig. 6) and that found by spectrometry of the intact TiNi-encapsulated seed (above). These determinations therefore were decidedly more uncertain (as reflected in their assessed uncertainties) than those for the assay of the master solution. The effect of these uncertainties, as propagated, on the uncertainties in the ^{32}P and ^{33}P assay results for the entire seed depended of course on the magnitude of f_{res}.

As given in Table 3, f_{res} for the four seeds ranged from a few tenths of a percent to over 7%. These values by themselves are deceptive in the sense that they do not reflect the ease with which the activity was extracted from the digested seeds. The digestions were performed over widely varying time periods (Table 1) and with vastly different numbers of repetitions of the solution transfers, rinses, bath replenishments, ultrasonic agitations, etc. As described in Section 2 and as illustrated in Fig. 5, the progress of each digestion was monitored so that the repetitive sequence of steps could be continued until it appeared that f_{res} had reached an acceptable level.

Seed P-97-15-2 was by far the most troublesome and its digestion required a modification to the procedure. After nearly two weeks of effort, less than 10% (i.e. $f_{res} \cong 0.9$) of the activity was extracted from the internal

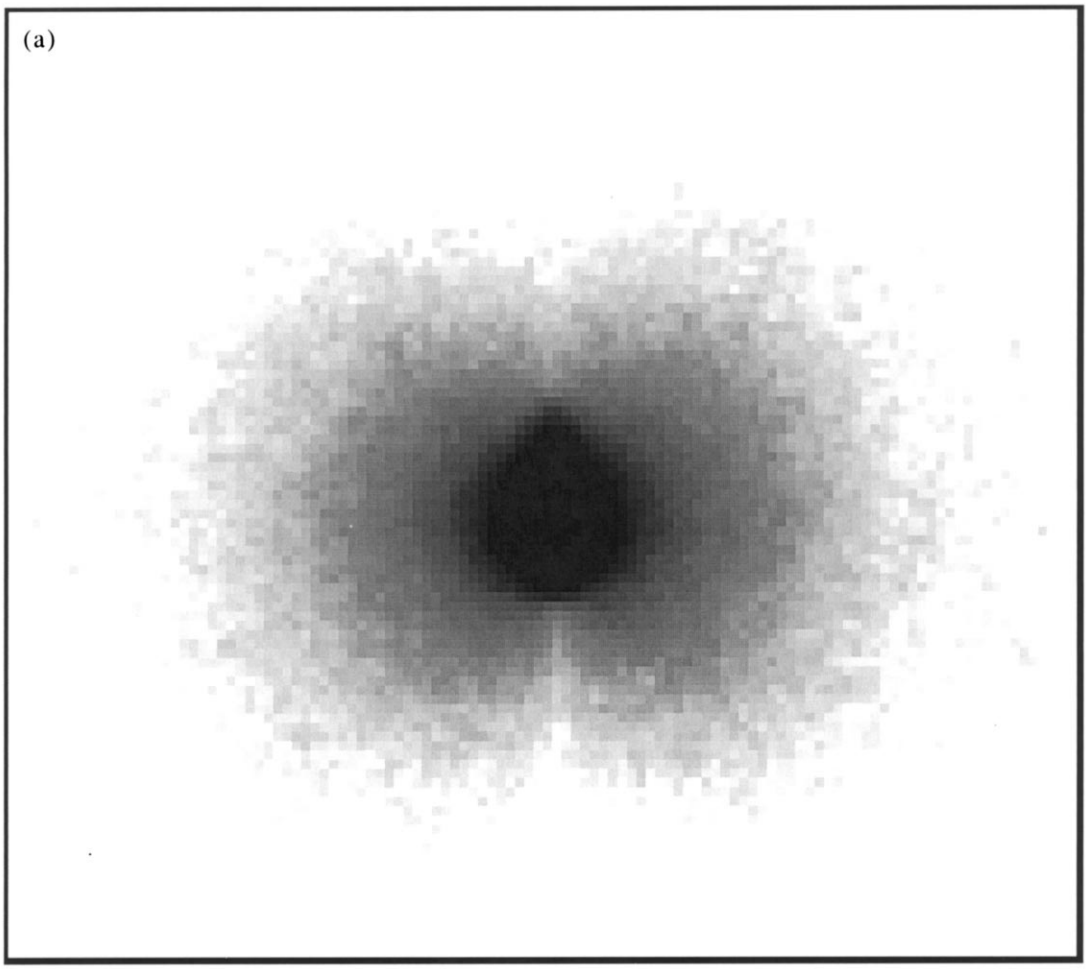

Fig. 9. Reproduction of the image obtained with an SSP imaging sensor from a 1-min exposure with seed #5. The butterfly-shaped gray pattern shows the radiation field emanating from and surrounding the seed; while the length of the small, central dark region (as micrometered) corresponds to its 3-mm active portion.

source material despite numerous ultrasonic agitation periods on nearly a daily basis. On continuation, it became apparent that the activity was being extracted at a very slow rate, and seemed to be reaching an asymptotically-approaching plateau of about 35% ($f_{res} \cong 0.65$). At this point, the remaining solid source material was cut into four nearly-equally-length pieces of about 7 mm each before continuing the extraction procedure. Ultimately, after cutting the source and after another two weeks of repetitive solution transfers, over 90% was finally extracted. The residual 8% ($f_{res} \cong 0.075 \pm 0.009$) was still too much activity for immediate determination by LS spectrometry, so the source had to be decayed (from counting rates of about 10^6 to around 10^3 s^{-1}). The difficulties encountered with this seed largely led to our understanding of the relation between the composition of the internal ^{32}P source material and the rate and ease of extracting the activity from it.

The other three seeds were, by comparison, relatively easy to extract. Yet, they too exhibited differences, most of which were somewhat understandable because of their known (but undisclosable) internal chemical composition. In order, the removal rate was probably fastest for the short seed #5, followed by P-97-23-6 and P-96-32-3. The larger f_{res} and larger relative uncertainty for seed P-97-23-6 were only a result of not making greater efforts to extract more of the activity (over a longer period) or expending the extra effort to determine f_{res} more precisely (at later decay times).

3.6. On the activity in adjacent TiNi-wire sections of the sources

The results for the fraction of activity in the cut-off sections (adjacent to the 'active seed' portions) of the originally-submitted wire sources are also presented in Table 3. A section from the 3-mm prototype seed #5

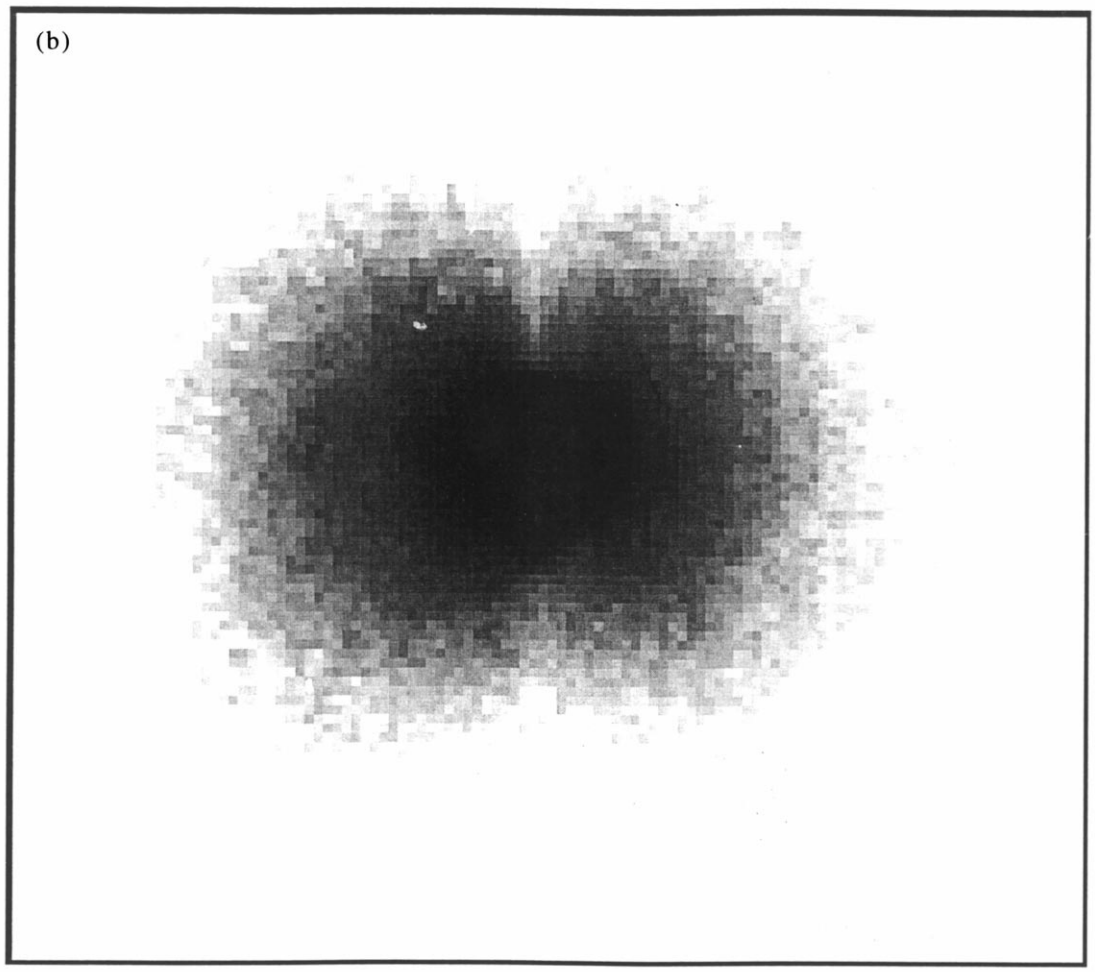

Fig. 9. Continued

was not available. Assayed sections of the other three 27-mm seeds varied in length from 7 to 20 mm (see Table 1).

The fractional activity in these three sections ranged from $2{\cdot}10^{-4}$ to $(8 \pm 3)10^{-8}$, with an intermediate value of $(6 \pm 2)10^{-7}$. It must be noted that the largest fraction (of 10^{-4} magnitude) is an upper bound and efforts were not made to determine the value more precisely (at a lower limit of detection).

The well localized containment of the activity in the 'active' 27-mm portions of the seeds, as evidenced by these results, largely confirms (by radioactivity measurements) the same results that were previously obtained from the dosimetric spatial distributions on these seeds (Soares, 1997), as well as from some cursory imaging done with a storage photostimulable phosphor (SSP) imager system on seed #5 and P-96-32-3. Cheng et al. (1996) described the use of such a system for radioactivity measurements. Fig. 9 shows the image obtained on a SSP imaging-sensor plate as obtained by an exposure with the 3-mm seed #5.

3.7. On the assessment of the uncertainties in the ^{32}P and ^{33}P activities and their ratios

The uncertainty assessments for both the ^{32}P activity and ^{33}P activity content of the seeds, as summarized in Tables 4 and 5, are somewhat straightforward. Examination of Eq. (2) indicates that one must consider the contributions due to the uncertainty in the aliquant masses m and in the lifetime intervals T (in forming R_i), as well as those for the efficiencies ϵ_{32} and ϵ_{33}, decay constants λ_{32} and λ_{33} and the determination of midpoint times t_i. The uncertainties in ϵ_{32} and ϵ_{33},

Table 4
Uncertainty assessment for ^{32}P activity at the certified reference times

Uncertainty component	Relative standard uncertainty (in percent)			
	source #5	source P-96-32-3	source P-97-15-2	source P-97-23-6
LS measurement precision and regression to resolve the ^{32}P and ^{33}P components[a]	1.3	0.097	1.5	0.21
Effect of ^{32}P half-life on regression result[b]	0.19	0.18	0.23	0.20
Effect of ^{33}P half-life on regression result[b]	0.47	0.12	0.68	0.070
Losses for the chemical digestion and solution transfers[c]	0.07	0.1	0.3[d]	0.1
Master solution gravimetric dilution	0.05	0.2	0.15	0.1
Correction for residual activity in undigested source	0.01	0.03	0.87	0.53
Correction for residual activity on tools	–	0.003	0.003[e]	0.02
Gravimetric preparation of LS counting sources	0.05	0.05	0.05	0.05
LS cocktail stability, composition and mismatch effects[f]	<0.1	<0.03	<0.02	<0.05
Counting lifetime determinations[g]	0.1	0.1	0.1	0.1
Effect of timing interval determinations on regression results[h]	0.17	0.031	0.073	0.032
Effect of ^{32}P detection efficiency on regression results[i]	0.41	0.32	0.31	0.34
Effect of ^{33}P detection efficiency on regression results[i]	3.6	0.068	0.20	0.048
Combined standard uncertainty	3.9	0.48	1.9	0.72
Expanded uncertainty ($k = 2$)	7.8	0.96	3.8	1.4

[a] See Table 1 for degrees of freedom in result.[b]The effects of the 0.098% relative uncertainty in the ^{32}P half-life and the 0.47% uncertainty in the ^{33}P half-life on the regression results depend on the ^{33}P/^{32}P activity ratios at the measurement times and on the time interval over which the measurements were performed.[c]Estimated from ^{32}P tracing experiments for each step of the established chemical digestion procedure (see Table 2).[d]The uncertainty estimate for losses in this case was somewhat arbitrarily increased by a factor of three since the procedure was modified. See footnote [h] of Table 3.[e]The uncertainty may be underestimated due to the need to cut the source into pieces during the chemical digestion. See footnote [h] of Table 3.[f]Estimated upper limits for the relative standard uncertainty based on systematic LS cocktail composition trends.[g]The lifetime of each counting cycle is determined by counting pulses from a gated crystal-controlled oscillator.[h]The timing uncertainty between intermittent LS measurement cycles, in terms of real clock times, is negligible. The cited uncertainty given here largely manifests as a result of an empirical correction that is applied to the LS spectrometer's internal elapsed time counter. The effects of these timing uncertainties on the regression results are dependent on the ^{33}P/^{32}P activity ratios at the measurement times and on the time intervals over which the LS measurements were performed.[i]The relative uncertainties in the ^{32}P and ^{33}P detection efficiency calculations themselves were typically in the range of 0.3 to 0.4% and included uncertainty contributions due to: the employed ^{3}H standard: quench indicating parameter (QIP) measurements; assumed beta maximum endpoint energies; calculational step sizes; fitted relations between the calculated efficiencies, QIP determinations and the EFFY4-code figures of merit; ionization quenching model assumptions and phototube response asymmetry. The resultant effects of these uncertainties on the regression results are dependent on the ^{33}P/^{32}P activity ratios at the measurement times and on the time intervals over which the LS measurements were performed.

Table 5
Uncertainty assessment for the ^{33}P activity at the certified reference times

Uncertainty component	Relative standard uncertainty (in percent)			
	source #5	source P-96-32-3	source P-97-15-2	source P-97-23-6
LS measurement precision and regression to resolve the ^{32}P and ^{33}P components[a]	0.19	0.47	1.3	1.8
Effect of ^{32}P half-life on regression result[b]	0.038	1.1	0.20	2.0
Effect of ^{33}P half-life on regression result[b]	0.67	0.73	0.70	0.67
Losses for the chemical digestion and solution transfers[c]	0.07	0.1	0.3[d]	0.1
Master solution gravimetric dilution	0.05	0.2	0.2	0.1
Residual activity in undigested source	0.01	0.03	0.87	0.53
Residual activity on tools	–	0.003	0.003[e]	0.02
Gravimetric preparation of LS counting sources	0.05	0.05	0.05	0.05
LS cocktail stability, composition and mismatch effects[f]	< 0.1	< 0.03	< 0.02	< 0.05
Counting lifetime determinations[g]	0.1	0.1	0.1	0.1
Effect of timing interval determinations on regression results[h]	0.034	0.19	0.069	0.30
Effect of ^{32}P detection efficiency on regression results[i]	0.050	1.6	0.51	2.6
Effect of ^{33}P detection efficiency on regression result[i]	0.43	0.34	0.33	0.36
Combined standard uncertainty	0.84	2.2	1.9	3.9
Expanded uncertainty ($k = 2$)	1.7	4.4	3.7	7.7

[a] through [h] are identical to those given in Table 4.

in turn, are comprised of many components as given in footnote (i) of Table 4 and were evaluated using the model developed by Collé and Zimmerman (1996b). The results for the Eq. (2) regression for the (R_i, t_i) data which yields the fitted parameters $A_{32(0)}$ and $A_{33(0)}$ for the master solution has a 'fitting' uncertainty, call it s_A, that fully embodies both the within-sample and between-sample LS measurement precision, and includes the variability in the background B_i determinations. Uncertainty components due to LS cocktail stability, composition and mismatch effects are evaluated separately (Zimmerman and Collé, 1997b; Collé, 1999). Lastly, one needs assessments due to the contributing uncertainties on the gravimetrically-determined master solution dilution, possible losses during the chemical digestion and solution transfers and corrections for the residual activity in the undigested portion of the seed and the residual activity on any transfer tools. Additional comments on these uncertainty components have been incorporated as notes to Table 4. Inspection of Tables 4 and 5 reveals that the more dominant uncertainty components, depending on conditions, are different for the ^{32}P and ^{33}P assessments and they vary amongst the four sources.

The uncertainty for the $^{33}P/^{32}P$ impurity ratio $I_0 = A_{33(0)}/A_{32(0)}$ cannot be directly obtained by combining the uncertainties in $A_{33(0)}$ and $A_{32(0)}$ since these two variables are highly correlated. The uncertainties in $A_{33(0)}$ and $A_{32(0)}$ as obtained from just the regression result are of such a nature that they are equal, irrespective of the magnitudes of $A_{33(0)}$ and $A_{32(0)}$. The regression's fitting uncertainty s_A (refer above) applies to both ^{33}P and ^{32}P, as a result of their Eq. (2) linear combination, so that their relative uncertainties are $s_A/A_{33(0)}$ and $s_A/A_{32(0)}$. One simple way to sort out this part of the correlation is to re-write Eq. (2) in terms of parameters $A_{32(0)}$ and I_0:

$$R_i = A_{32(0)}[\epsilon_{32} \exp(-\lambda_{32} t_i) + I_0 \epsilon_{33} \exp(-\lambda_{33} t_i)] \quad (6)$$

and to the fit the (R_i, t_i) data to the Eq. (6) nonlinear-combination functional form. In this way, a separate fitting uncertainty in I_0 can be directly obtained from the regression results. The correlation also occurs because many of the contributing sources of uncertainty are wholly common, with an exact correlation coefficient of unity. These components include: the uncertainty contributions due to any chemical-digestion or solution-transfer losses, dilution of the master solution, any corrections for residual activities either in the remaining portion of the seed or on the tools, aliquant masses used to form the LS cocktails, and counting lifetime determinations. Lastly, one has the partial correlation in the ϵ_{32} and ϵ_{33} efficiency terms whose values were obtained from common algorithmic assumptions and calculations. The uncertainty assessment for the impurity ratio I_0, which has removed the ^{32}P and ^{33}P activity determination correlations, is given in Table 6.

3.8. On the $^{33}P/^{32}P$ impurity ratios

What might be termed 'initial' $^{33}P/^{32}P$ impurity ratios I_X for the four seeds were obtained by decay correcting the I_0 assay results at their T_0 reference

Table 6
Uncertainty assessment for the $^{33}P/^{32}P$ activity ratio at the certified reference times

Uncertainty component	Relative standard uncertainty (in percent)			
	source #5	source P-96-32-3	source P-97-15-2	source P-97-23-6
LS measurement precision and regression to resolve the ^{32}P and ^{33}P components[a]	1.3	0.56	2.0	1.8
Effect of ^{32}P half-life on regression result[b]	0.038	1.3	0.20	2.0
Effect of ^{33}P half-life on regression result[b]	0.67	0.86	0.70	0.67
Effect of timing interval determinations on regression result[c]	0.034	0.22	0.069	0.30
Effect of ^{32}P detection efficiency on regression result[d]	0.050	1.6	0.51	2.6
Effect of ^{33}P detection efficiency on regression result[d]	0.43	0.34	0.33	0.36
Combined standard uncertainty	1.5	2.3	2.2	3.8
Expanded uncertainty ($k = 2$)	3.0	4.7	4.4	7.7

[a] See Table 1 for degrees of freedom in result.[b]See note [b] in Table 4.[c]See note [h] in Table 4.[d]See note [i] in Table 4.

times (Table 3 and 7) to the earliest reported Guidant reference times T_X. It is presumed that the T_X values represent times that might be considered to approximate that for freshly-prepared ^{32}P source material. The decay-corrected I_X values range $0.008 \leq I_X \leq 0.016$ which are entirely consistent with previous observations (refer to Collé (1997a,c) and the discussion in Section 1) that typically $I_X \leq 0.008$, particularly considering that T_X may in some cases be at least a few weeks later than the actual ^{32}P production times.

3.9. On the comparison of the ^{32}P assay results with Guidant reported activities

A comparison of the decay-corrected, NIST-certified ^{32}P activities A_{NIST} for the four seeds with the activities A_X initially reported by Guidant is summarized in Table 8. As discussed previously, A_X for seed #5 was reported with respect to both of their preliminary calibration methods and differed by about 25 to 30%. The values of A_X for all three 27-mm seeds were given only with respect to their LS calibration values (which was used to establish a calibration factor for their well counter). It should be noted that the apparent discrepancy in two values for seed P-97-15-2 (as pointed out in footnote (b) of Table 1) is believed to be merely a result of a transcription error for the first.

The consistent results in A_X/A_{NIST} for the three 27-mm seeds are useful in showing the good agreement amongst the NIST assay results which were obtained under a wide variety of different conditions (activity and impurity levels, residual activities, internal source compositions, digestion times, measurement times, decay intervals, etc.). In a way, one could consider the Guidant measurements to be an independent check on the consistency in the NIST assay results. In fact, these results, which have a range $1.50 \leq A_X/A_{NIST} \leq 1.54$, exhibit greater reproducibility than that obtained by NIST from ionization current measurements on two of the seeds using a commercial, 'dose calibrator' type, re-entrant ionization chamber (Collé et al., 1999).

Table 7
Comparison of the 'initial' $^{33}P/^{32}P$ impurity ratios

Source identification	NIST reference time, T_0^a	Guidant reference time (earliest reported), T_X^b	$^{33}P/^{32}P$ activity ratio at time T_0^a	$^{33}P/^{32}P$ activity ratio at time T_X^c
#5	1200 EST 1 December 1996	29 January 1996[d]	7.186 ± 0.219	0.0106 ± 0.0009
P-96-32-3	1200 EST 14 January 1997	1100 EST 26 August 1996	0.1720 ± 0.0080	0.0086 ± 0.0005
P-97-15-2	1200 EST 22 August 1997	1100 EST 20 February 1997	0.4131 ± 0.0183	0.0157 ± 0.0016
P-97-23-6	1200 EST 6 October 1997	1100 EST 6 June 1997	0.1107 ± 0.0085	0.0083 ± 0.007

[a] See Table 3.[b]See Table 1.[c]Assuming the ^{32}P and ^{33}P half-lifes given in Table 1. The cited uncertainty intervals are for a $k = 2$ coverage factor and include the additional uncertainty components for the ^{32}P and ^{33}P decay corrections from time T_0 to time T_X.[d] Assumed to be at 1200 EST.

Table 8
Comparison of the ^{32}P assay results with the reported activities

Source identification	Guidant reference time, T_X	Guidant reported ^{32}P activity A_X at time T_X (Bq)	NIST ^{32}P activity A_{NIST} decay corrected to time T_X^a (Bq)	A_X/A_{NIST}^b
#5	29 January 1996[c]	$5.946(10^9)$	$(3.031 \pm 0.253)10^9$	1.962 ± 0.164
	31 January 1996[c]	$5.339(10^9)$	$(2.751 \pm 0.229)10^9$	1.941 ± 0.162
	1 February 1996[c]	$5.080(10^9)$	$(2.620 \pm 0.218)10^9$	1.939 ± 0.162
	5 February 1996[c]	$4.233(10^9)$	$(2.157 \pm 0.179)10^9$	1.962 ± 0.163
	6 February 1996[c]	$4.000(10^9)$	$(2.055 \pm 0.171)10^9$	1.947 ± 0.162
#5 (LS)	25 September 1996[c]	$4.015(10^4)$	$(2.606 \pm 0.204)10^4$	1.541 ± 0.121
P-96-32-3	1100 EST 26 August 1996	$1.277(10^9)$	$(8.294 \pm 0.137)10^8$	1.540 ± 0.026
P-97-15-2	1100 EST 20 February 1997	$1.236(10^{10})$	$(8.844 \pm 0.370)10^9$	1.398 ± 0.059[d]
	0830 EST 2 April 1997	$1.817(10^9)$	$(1.212 \pm 0.489)10^9$	1.499 ± 0.061
P-97-23-6	1100 EST 6 June 1997	$8.114(10^9)$	$(5.330 \pm 0.099)10^9$	1.522 ± 0.028

[a] From the ^{32}P activity values given in Table 3 with decay corrections to T_X using a half-life of 14.262 ± 0.014 d. The cited uncertainty intervals are for a $k = 2$ coverage factor and include the additional uncertainty component for the ^{32}P decay correction to time T_X.[b]The cited uncertainty intervals are for a coverage factor of $k = 2$ and reflect only the uncertainties in the A_{NIST} determinations.[c]The times on the given dates are assumed to be at 1200 EST.[d]The apparent 7% difference in decay-corrected reported activities was identified in footnote [b] of Table 1.

Another interesting point may be useful for other researchers to consider. Well-chamber ionization current measurements of the seeds by comparisons to a ^{32}P solution standard (as for Guidant's first preliminary calibration) were decidedly worse (yielding results in error by nearly a factor of two) than the second LS spectrometry approach (which had to employ an educated (or calculated) guess at the LS efficiency for the intact seeds). The previously given NIST results for the LS spectrometry of intact seeds (see above) may suggest a plausible reason for why the estimated LS efficiency wasn't calculated (or guessed at) very well. Calculations show that only about 70% of the ^{32}P β spectrum exits the seed's TiNi encapsulation, yet the effective LS efficiency for the intact seeds was found to be over 90%. Application of this (0.7/0.9) factor to the $A_X/A_{NIST} \cong 1.5$ result moves the comparison ratio much closer to unity, and agreement between the two sets of measurements.

Based on the findings summarized in Table 8, Guidant was able to establish a very accurately-determined calibration factor for their quality control measurements, which they immediately effected.

Collé et al. (1998), in a companion paper, also used the results of the present work to establish a 'dial setting' calibration factor for the non-destructive assay of these Guidant seeds by measurements with a widely-available, commercial 'dose calibrator'.

4. Concluding notes

The development and deployment of this chemical digestion and radionuclidic assay procedure for determining the ^{32}P content of the TiNi-encapsulated Guidant intravascular brachytherapy sources were critical in linking the necessary dosimetric measurements and calculations. The results also established non-destructive calibration factors for the manufacturer's in-house quality control, as well as for a widely-available, commercial, ionization-chamber-based instrument (which is being reported on elsewhere).

The method and results are, of necessity, unique and specific to their application to the Guidant sources. Nevertheless, the generalized approach used here, i.e. in terms of first understanding the underlying radiochemistry, designing a complementary detailed procedure and coupling it to world-class radionuclidic metrology, may be quite applicable to the development of comparable procedures for other such sealed sources that need to be assayed by destructive means. In fact, work (based on the same principles) for the assay of stainless-steel-encapsulated, ceramic-based $^{90}Sr/^{90}Y$ intravascular brachytherapy sources is currently underway at NIST.

Acknowledgements

The National Institute of Standards and Technology (NIST) is an agency of the Technology Administration of the US Department of Commerce. Certain commercial equipment, instruments and materials are identified in this paper to foster understanding. Such identification does not imply recommendation or endorsement by NIST, nor does it imply that the materials or equipment identified are the best available for the purpose. This work was financially supported in part by Guidant Intravascular Intervention (Houston, TX) for

the calibration tests and radionuclidic assays that were provided by NIST on a fee basis. The author thanks his esteemed colleagues, B.E. Zimmerman, B.M. Coursey, C.G. Soares and S. Seltzer, for their encouragements and helpful commentaries on this work. Several other contributors to this work must be credited: S. Lott and K. Bueché (Guidant) for their enthusiastic support and for their co-operation in willingly providing the confidential information on the internal compositions of the sources (without which the digestion procedure could not have been as easily devised); F.J. Schima (NIST) for performing the photonic-emission-spectrometry impurity analyses and S. Seltzer (NIST) for his calculations of the ^{32}P and ^{33}P beta spectra for the TiNi-encapsulated seeds.

References

AHA (American Heart Association), 1997. Heart and Stroke A–Z Guide: Cardiovascular Disease Statistics. AHA, Washington, DC.

Barksdale, J., 1953. Handbook on Titanium. Titanium Metals Corp. of America, p. 46.

Cheng, Y.T., Soodprasert, T., Hutchinson, J.M.R., 1996. Radioactivity using storage phosphor technology. Appl. Radiat. Isot. 47, 1023–1031.

CIRMS (Council on Ionizing Radiation Measurements), 1998. Report on National Needs in Ionizing Radiation Measurements. CIRMS Science and Technology Committee, Gaithersburg, MD.

Collé, R., 1993. Long-term stability of carrier-free polonium solution standards. Radioact. Radiochem. 4 (1), 20–35.

Collé, R., Thomas, J.W., L, 1993. $^{36}Cl/Cl$ Accelerator-mass-spectrometry standards: verification of their serial-dilution-solution preparations by radioactivity measurements. J. Res. Natl. Inst. Stand. Tech. 98, 653–677.

Collé, R., Zhichao, L., Hutchinson, J.M.R., Schima, F.J., 1994. Delayed isomeric state in ^{205}Pb and its implications for the $4\pi\alpha$ liquid scintillation spectrometry of ^{209}Po. Appl. Radiat. Isot. 45, 1165–1175.

Collé, R., 1995. A precise determination of the ^{222}Rn half-life by 4π–$\alpha\beta$ liquid scintillation measurements. Radioact. Radiochem. 6 (1), 16–29.

Collé, R., Zhichao, L., Schima, F.J., Hodge, P.A., Thomas, J.W.L., Hutchinson, J.M.R., Coursey, B.M., 1995. Preparation and calibration of carrier-free ^{209}Po solution standards. J. Res. Natl. Inst. Stand. Tech. 100, 1–36.

Collé, R., Zimmerman, B.E., 1996a. ^{63}Ni Half-life: a new experimental determination and critical review. Appl. Radiat. Isot. 47, 677–691.

Collé, R., Zimmerman, B.E., 1996b. Nickel-63 standardization: 1968–1995. Radioact. Radiochem. 7 (2), 12–27.

Collé, R., 1997a. A simple transform to linearize and resolve two-component decay data: illustration of its use and efficacy in assaying $^{33}P/^{32}P$ mixtures by liquid scintillation counting. Radioact. Radiochem. 8 (2), 5–18.

Collé, R., 1997b. Systematic effects of total cocktail mass (volume) and H_2O fraction on $4\pi\beta$ liquid scintillation spectrometry of ^{3}H. Appl. Radiat. Isot. 48, 815–831.

Collé, R., 1997c. Cocktail mismatch effects in $4\pi\beta$ liquid scintillation spectrometry: implications based on the systematics of ^{3}H detection efficiency and quench parameter variations with total cocktail mass (volume) and H_2O fraction. Appl. Radiat. Isot. 48, 833–842.

Collé, R., Kishore, R., 1997. An update on the NIST radon-in-water standard generator: its performance efficacy and long-term stability. Nucl. Instrum. Methods Phys. Res. A 391, 511–528.

Collé, R., Zimmerman, B.E., 1997. A compendium on the NIST radionuclidic assays of the massic activity of ^{63}Ni and ^{55}Fe solutions used for an international intercomparison of liquid scintillation spectrometry techniques. J. Res. Natl. Inst. Stand. Tech. 102, 523–549.

Collé, R., 1999. Cocktail composition effects in low-energy liquid scintillation spectrometry: cocktail stability, tractability and mismatch effects. Submitted for publication.

Collé, R., Zimmerman, B.E., Soares, C.G, Coursey, B.M., 1998. Determination of a calibration factor for the non-destructive assay of Guidant ^{32}P intravascular brachytherapy sources. Appl. Radiat. Isot. 50, 835–841.

Cotton, F.A., Wilkinson, G., 1966. Advanced Inorganic Chemistry: A Comprehensive Text. Interscience Publ., NY, p. 492 ff.

Coursey, B.M., Grau Malonda, A., Garcia-Torano, E., Los Arco, J.M., 1985. Standardization of pure-beta-particle emitting radionuclides. Trans. Am. Nucl. Soc. 50, 13.

Coursey, B.M., Mann, W.B., Grau Malonda, A., Garcia-Torano, E., 1986. Standardization of carbon-14 by $4\pi\beta$ liquid scintillation efficiency tracing with hydrogen-3. J. Appl. Radiat. Isot. 37, 403.

Coursey, B.M., Lucas, L.L., Grau Malonda, A., Garcia-Torano, E., 1989. The standardization of plutonium-241 and nickel-63. Nucl. Instrum. Methods 112, 197–202.

Coursey, B.M., Cessna, J., Lucas, L.L., Garcia-Torano, E., Golas, D.B., Grau Malonda, A., Hoppes, D.D., Los Arcos, J.M., Martin-Casallo, M.T., Schima, F.J., Unterweger, M.P., 1991. The standardization and decay scheme of rhenium-186. Appl. Radiat. Isot. 42, 865–869.

Coursey, B.M., Calhoun, J.M., Cessna, J., Golas, D.B., Schima, F.J., Unterweger, M.P., 1994. Liquid-scintillation counting techniques for the standardization of radionuclides used in therapy. Nucl. Instrum. Methods Phys. Res. A 339, 26–30.

Coursey, B.M., Collé, R., Zimmerman, B.E., Cessna, J., Golas, D.B., 1998. National radioactivity standards for beta-emitting radionuclides used in intravascular brachytherapy. Int. J. Radiat. Oncol. Biol. Phys., 41, 207–216.

ENSDF (Evaluated Nuclear Structure Data File), 1997. On-Line Database. National Nuclear Data Center, Brookhaven National Laboratory, Upton, NY.

Garcia-Torano, E., 1993. Private communication on EFFY4. Centro de Investigaciones Energeticas, Medioambientales y Technologicas (CIEMAT), Madrid.

Garcia-Torano, E., Grau Malonda, A., 1985. EFFY: a new program to compute the counting efficiency of beta par-

ticles in liquid scintillators. Comput. Phys. Comm. 36, 307–312.

Grau Malonda, A., Garcia-Torano, E., 1982. Evaluation of counting efficiency in liquid scintillation counting of pure β-ray emitters. Int. J. Appl. Radiat. Isot. 46, 799–803.

Grau Malonda, A., Garcia-Torano, E., Los Arcos, J.M., 1985. Liquid scintillation counting efficiency as a function of the figure of merit for pure beta-particle emitters. Int. J. Appl. Radiat. Isot. 36, 157–158.

Landis, V.J., Kaye, J.H., 1971. Radiochemistry of Titanium, National Academy of Sciences and National Research Council Nuclear Science Series NAS-NS-3034 (Rev.). Published by US Atomic Energy Commission, Washington, DC.

Lott, S., 1997. Private communication. Guidant Vascular Intervention, Houston, TX.

NIST (National Institute of Standards and Technology), 1991. Certificate, Standard Reference Material 4927E, Hydrogen-3 Radioactivity Standard. Gaithersburg, Maryland.

NIST (National Institute of Standards and Technology), 1997. Report of Test to NeoCardia (Houston, TX). ^{32}P Beta-particle Wire Source S/N P-96-32-3. Gaithersburg, MD.

Schima, F.J., 1996. Private communication. National Institute of Standards and Technology, Gaithersburg, MD.

Seltzer, S., 1997. Private communication. National Institute of Standards and Technology, Gaithersburg, MD.

Soares, C.G., 1997. Private communication. National Institute of Standards and Technology, Gaithersburg, MD.

Taylor, B.N., Kuyatt, C.E., 1994. Guidelines for Evaluating and Expressing the Uncertainty of NIST Measurement Results, 1994 ed. Technical Note 1297. National Institute of Standards Technology (NIST), US Government Printing Office, Washington, DC.

Zimmerman, B.E., Collé, R., 1997a. Cocktail volume effects in 4πβ liquid scintillation spectrometry with ^{3}H-standard efficiency tracing for low-energy β-emitting radionuclides. Appl. Radiat. Isot. 48, 365–378.

Zimmerman, B.E., Collé, R., 1997b. Standardization of ^{63}Ni by 4πβ liquid scintillation spectrometry with ^{3}H-standard efficiency tracing. J. Res. Natl. Inst. Stand. Tech. 102, 455–477.

Zimmerman, B.E., Collé, R., 1997c. Comparison of the French and US National ^{3}H (tritiated H_2O) standards by 4πβ liquid scintillation spectrometry. Appl. Radiat. Isot. 48, 521–526.